Introduction and overview of biosensors

Prof. Dr. İsmail Hakkı Boyacı
Hacettepe University,
Food Reseach Center, Ankara, Turkey
ihb@hacettepe.edu.tr

"Phototech for Biosensors and Energy" 21-25 October 2013 Vouliagmeni, Athens, Greece

Nanoparticles

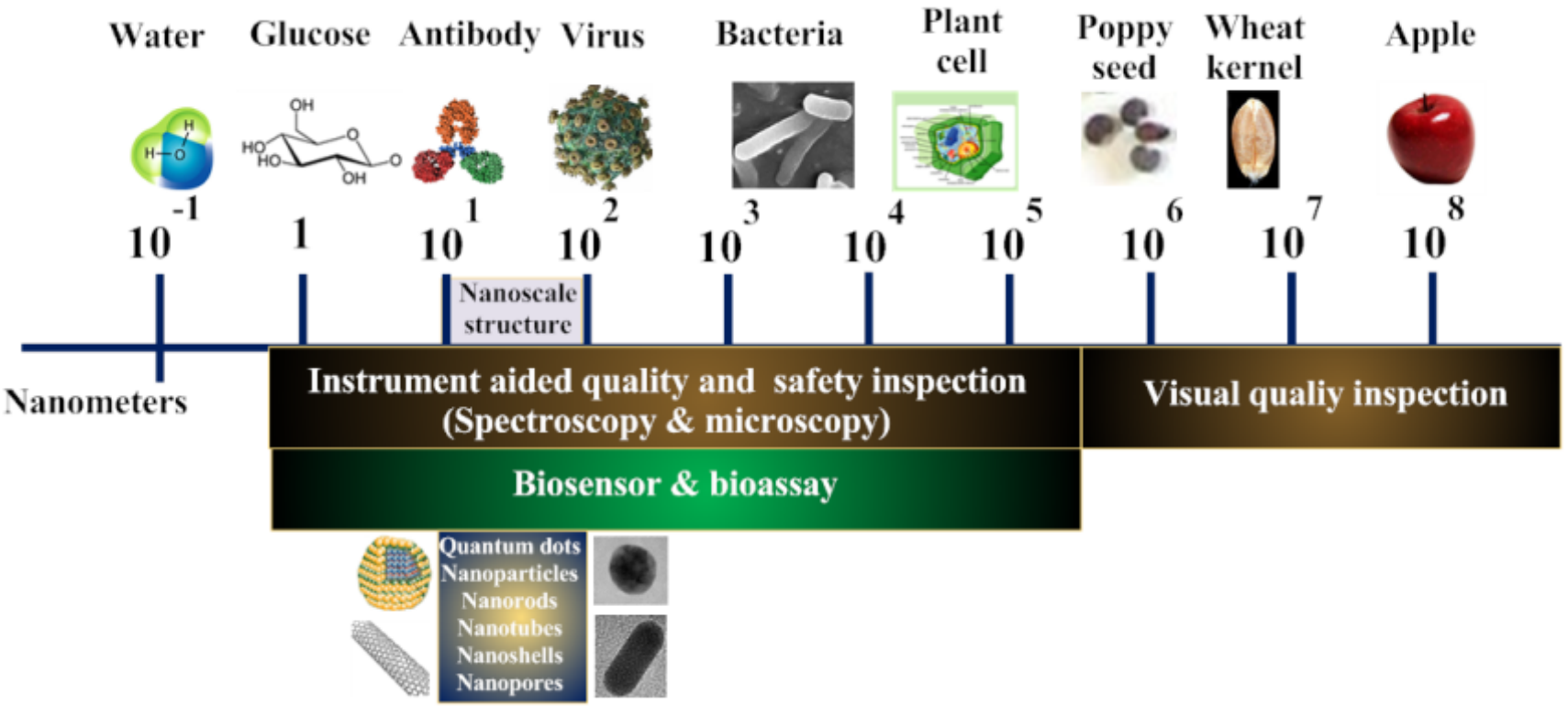

Metallic nanoparticle

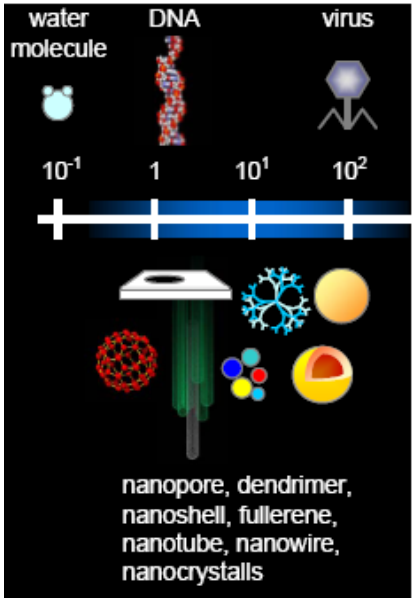

- Noble metals (Au, Ag);
- Magnetic materials (Fe_3O_4, Fe_3S_4, Fe_2O_3, $MO{\cdot}Fe_2O_3$, where M = Ni, Co, Zn, Mn, Mg);
- Semiconductor materials (CdS, CdSe, CdTe, ZnSe, PbS, PbTe);

Physical, electrical, optical, mechanical properties

- Tunable size
- Thermal stability
- High surface area
- Large pore volume per unit mass
- Suitable for sensor fabrication

Core-Shell nanoparticles

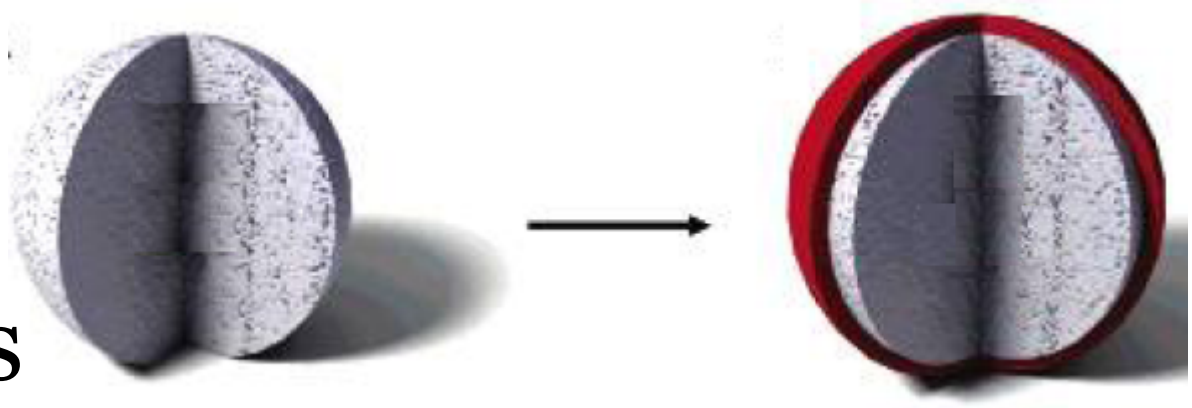

Schematic illustration of iron oxide spheres coated with an outer shell of gold

Core-Shell Fe_3O_4@Au

Core-Shell Fe_3O_4@CdTe

Core-Shell Fe_3O_4@silica

1) Synthesis of Fe_3O_4 nanoparticles

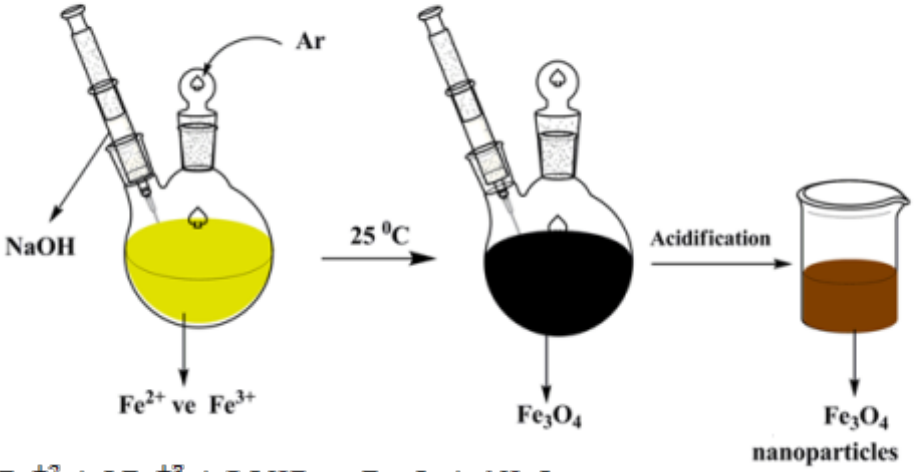

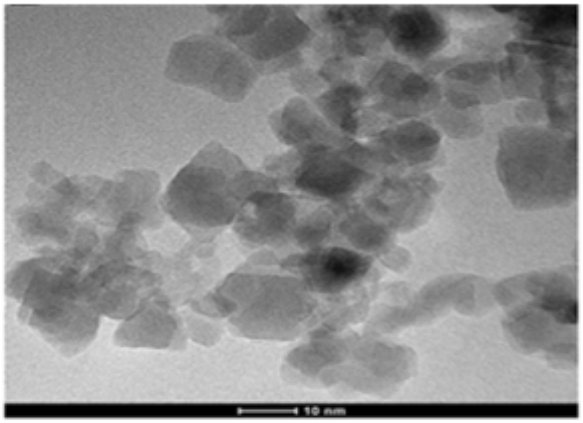

$$Fe^{+2} + 2Fe^{+3} + 8OH^- \rightarrow Fe_3O_4 + 4H_2O$$

2) Synthesis of spherical Fe_3O_4@ Au core-shell nanoparticles

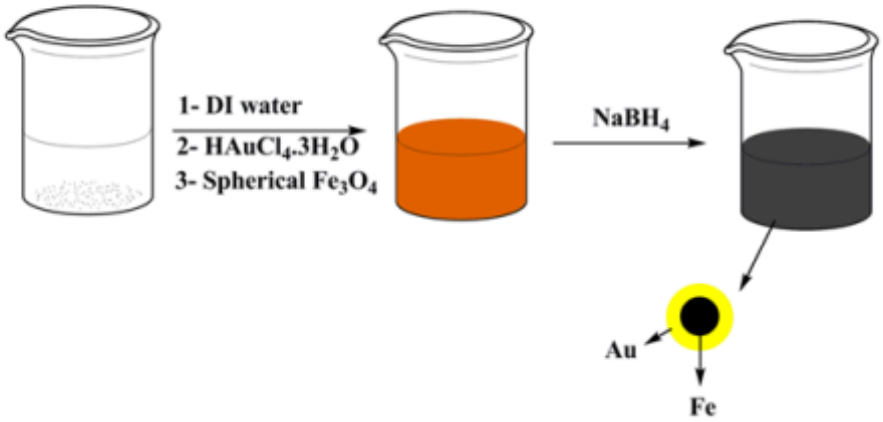

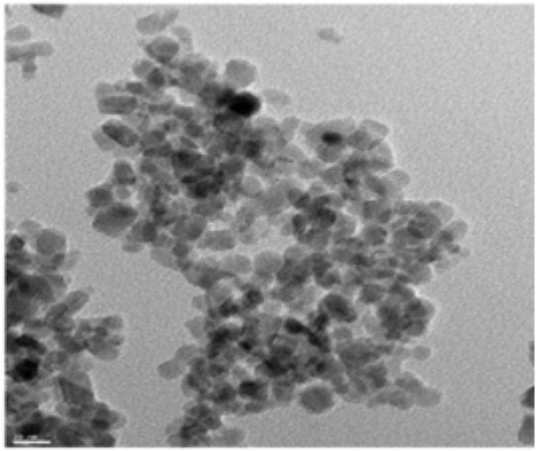

Uğur Tamer et al., J Nanoparticle Research (2010) 12:1187–1196

Synthesis of magnetic core–shell Fe_3O_4–Au nanoparticle

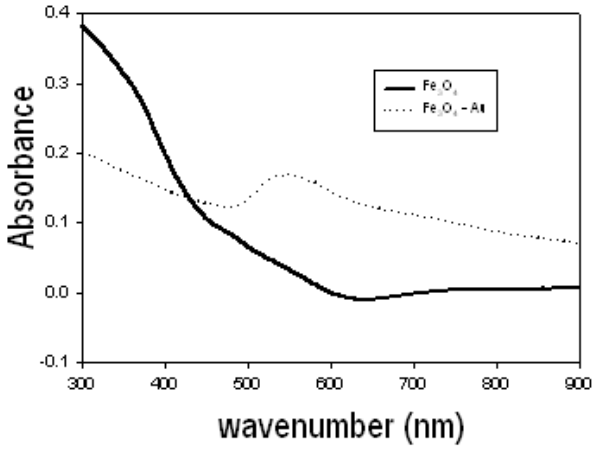

UV–Vis spectra of Fe_3O_4 and Fe_3O_4–Au nanoparticles

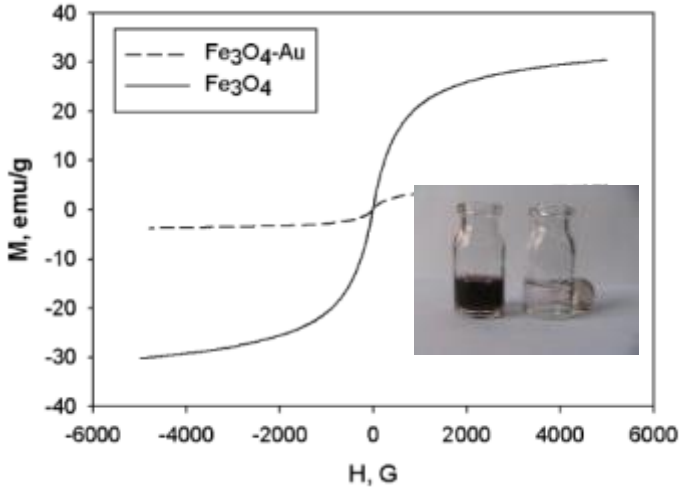

Hysteresis loops of Fe_3O_4 (solid line) and Fe_3O_4–Au (dotted line) nanoparticles

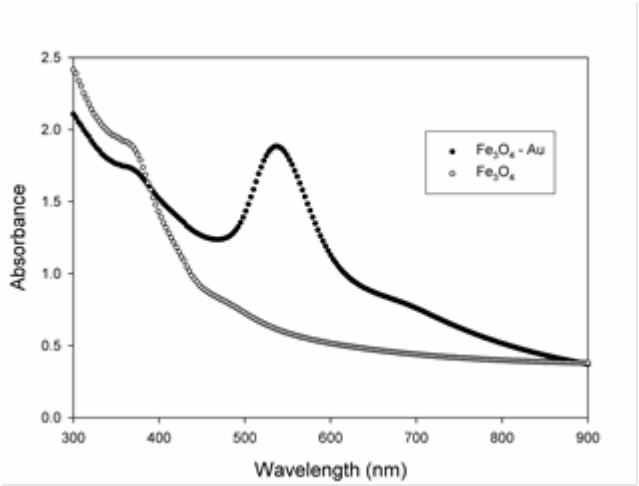

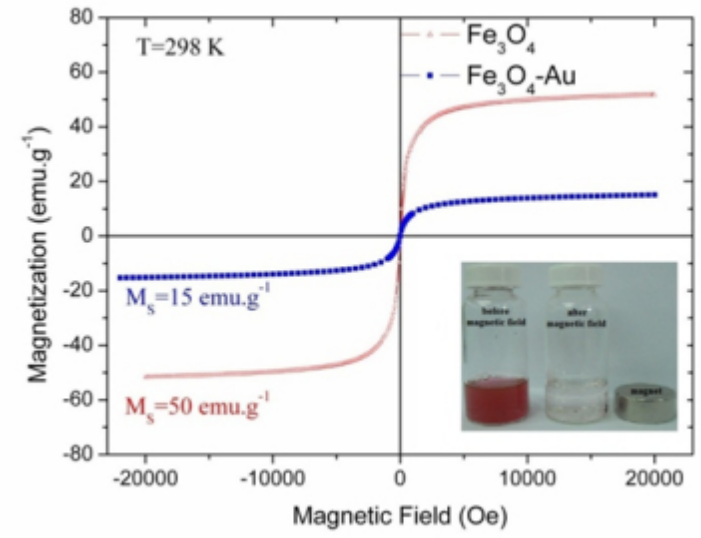

TEM images of anisotropic Fe_3O_4 @ Au core-shell nanoparticles

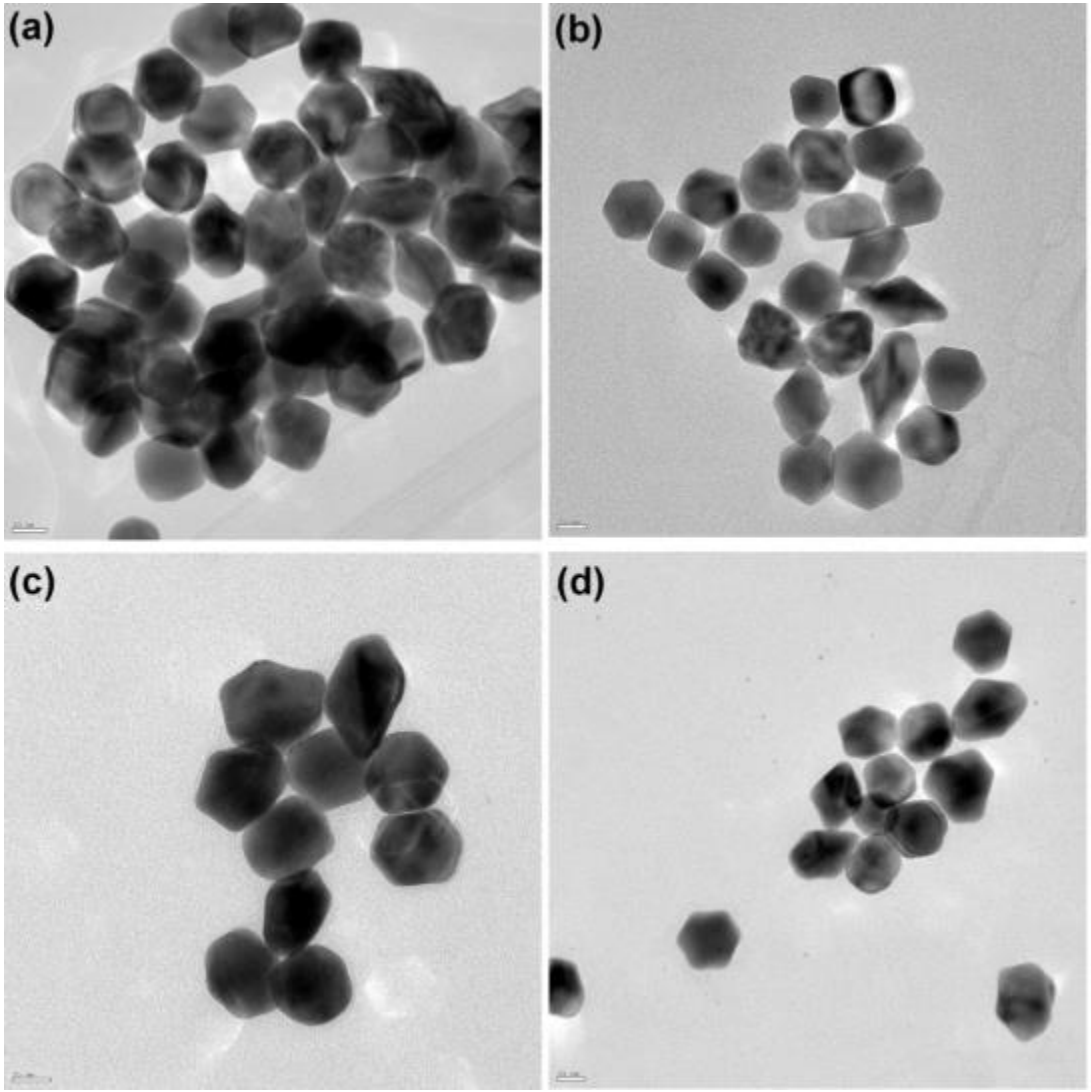

To demonstrate the viability of the gold iron nanoparticles for magnetic bioseparation,

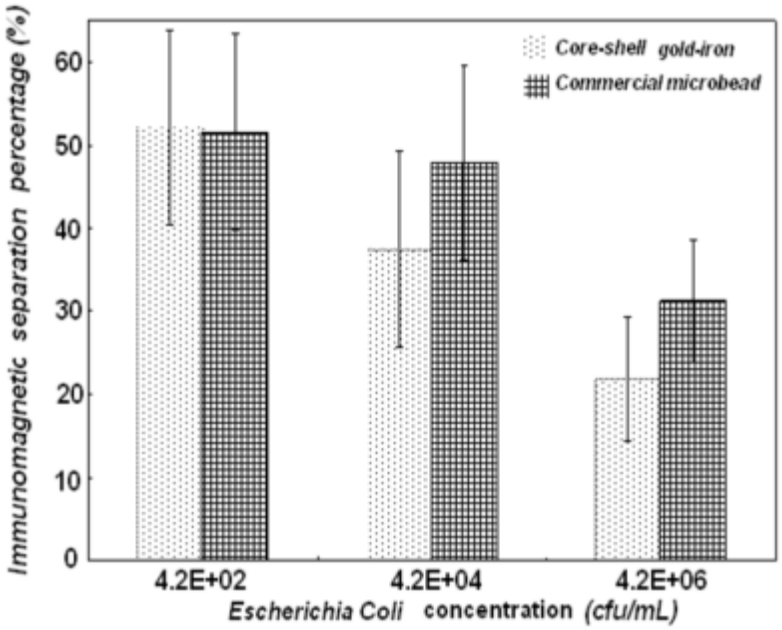

Comparison of magnetic bioseparation using gold-iron nanoparticles and commercial macromagnetic particles

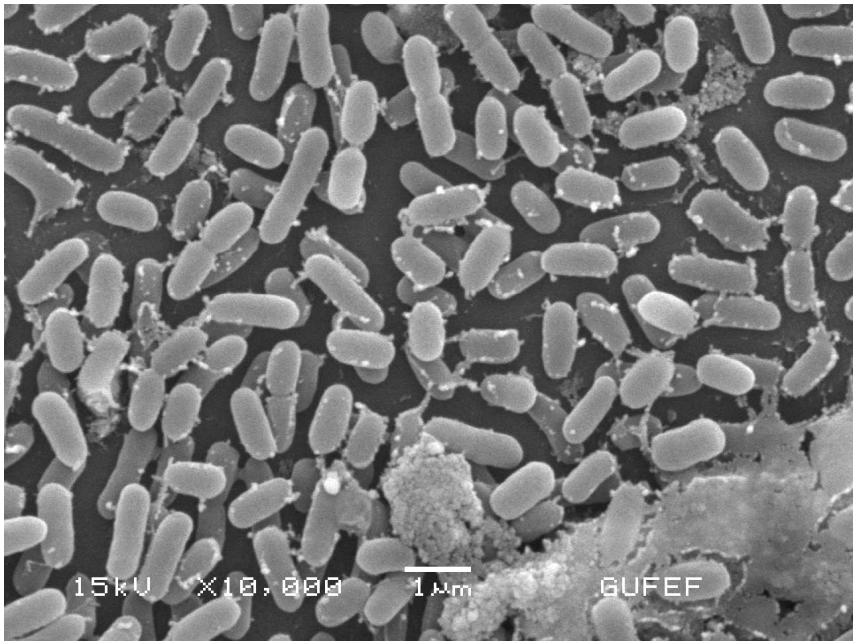

The antibody immobilized Fe_3O_4 nanoparticles were reacted with *E. coli*. A magnetic field was applied to collect the magnetically active bacteria.

Synthesis of anisotropic nanoparticles

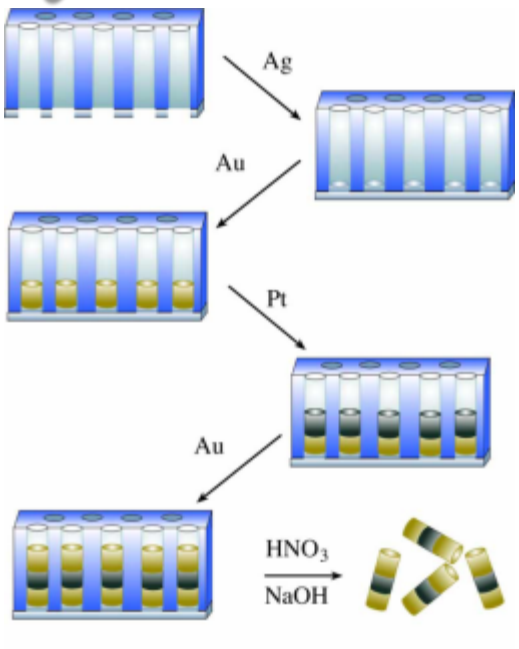

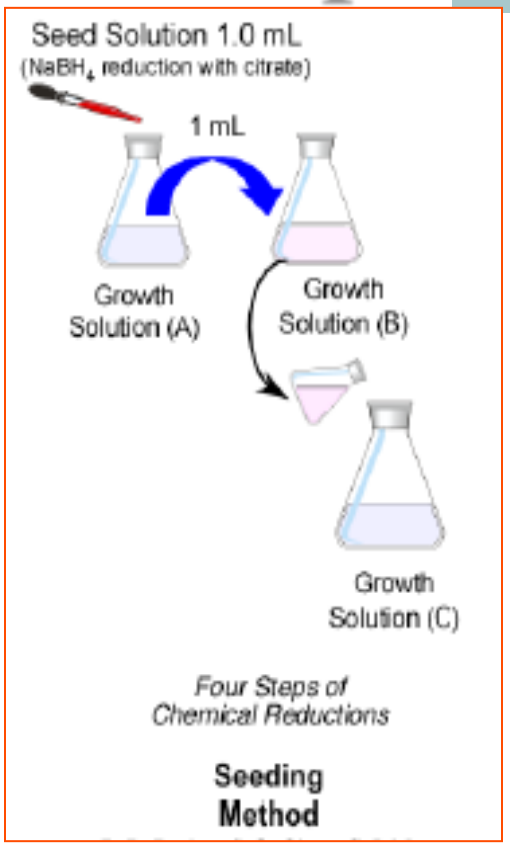

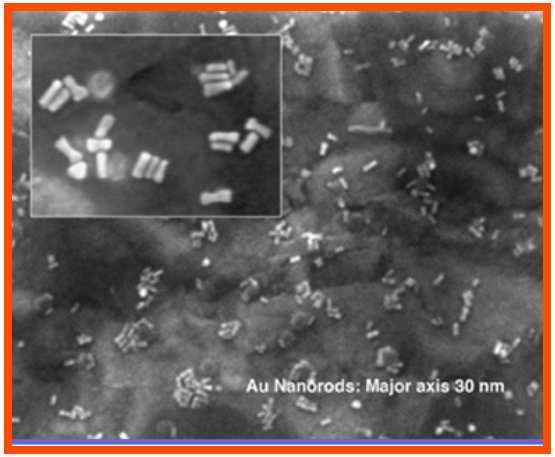

Erhan Temur, İsmail Hakkı Boyacı, Uğur Tamer et al., Anal Bioanal Chem (2010) 397:1595–1604

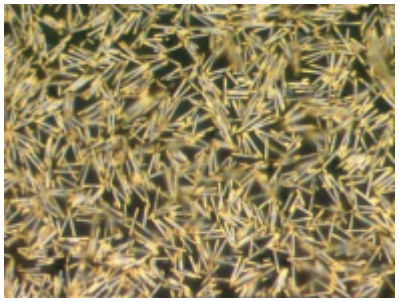

Au, Pt, Au nanowires that are 200 nm in diameter and 5 microns long

Brian D. Reiss, et al., Mat. Res. Soc. Symp. 2001 Vol. 635 C6.2.1

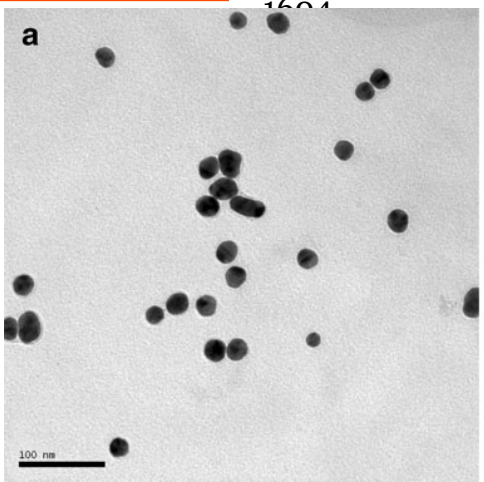

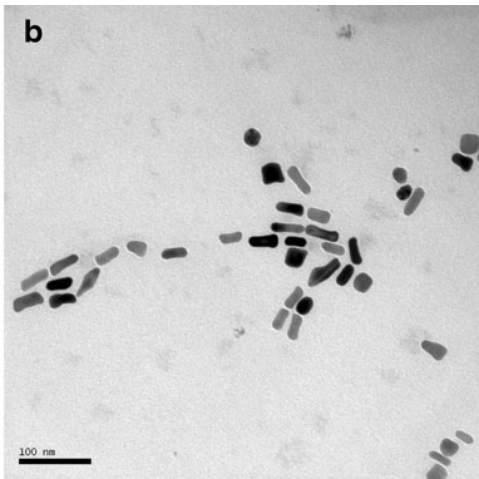

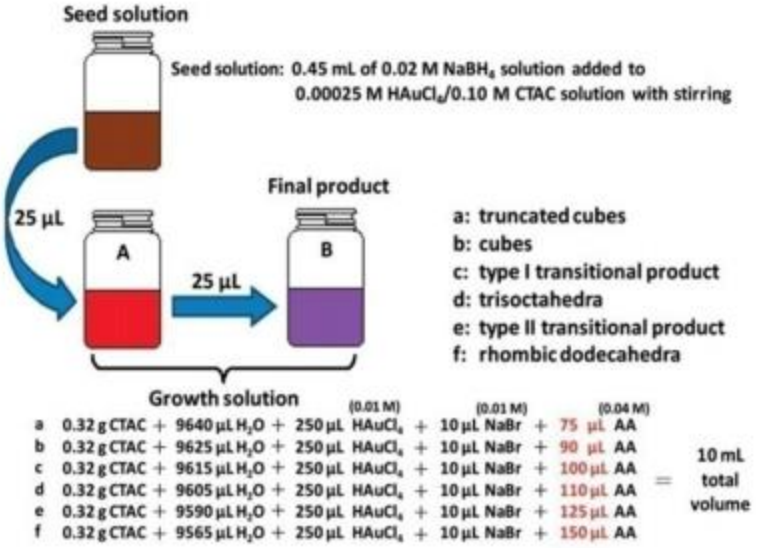

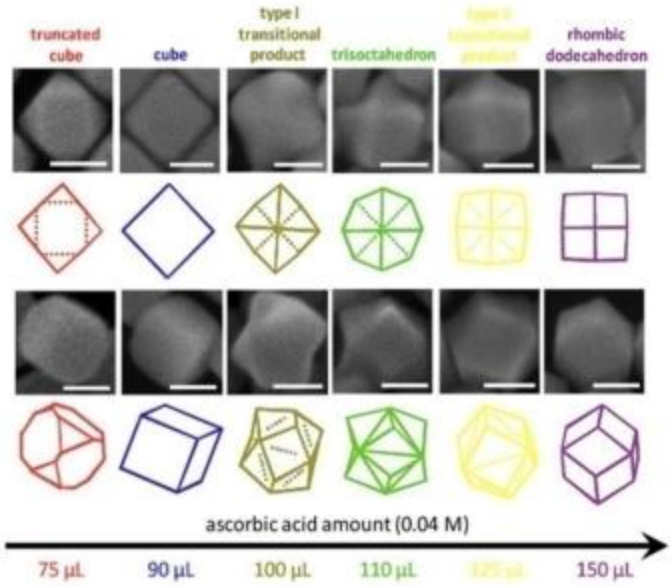

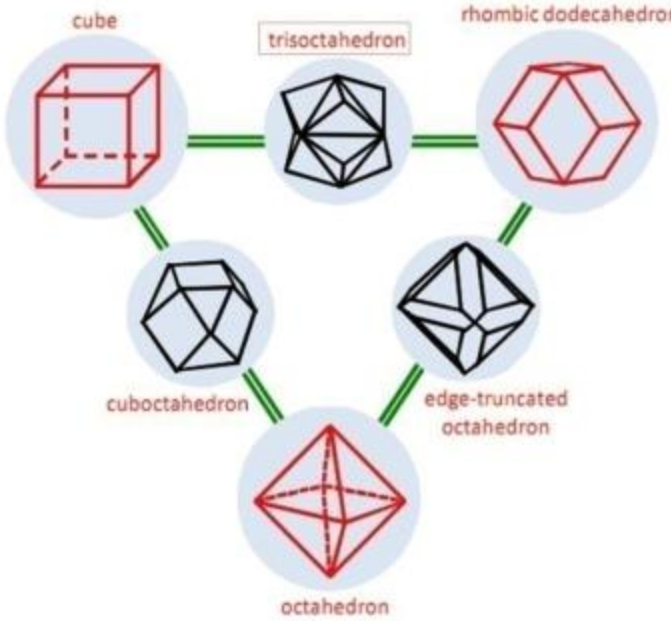

Wu HL et al., Langmuir, 2010, 26(14), 12307

Biosensor & Bioassay

Biosensors & Bioassays are methods that can determine the concentration of targets or biological activity of a substance such as enzyme, vitamin, hormone and plant growth factor using a bioreceptor. Biosensors & Bioassays may be qualitative or quantitative.

Biosensors generally employed on..

- Chemical method is either;
  - not available,
  - if available, too complex,
  - insensitive to low doses,
- Unknown chemical composition,
- Estimate the activity of the target,
- Measure the target toxicity,
- Quantity of the sample is to small,
- Purification for chemical assay not possible,
- Field analysis is need.

Bioreceptors

- A bioreceptor is a biological molecular spices (antibody, enzyme, protein, nucleic acid) a living biological system (cell, tissue or organisms) that utilizes a biochemical mechanism for recognition.
- Bioreceptors allow binding the specific analyte of interest to the assay for the measurement with the minimum interference from other components in the complex mixtures.
- The specificity of the bioassay is based on the bioreceptors used.

Most common forms of bioreceptors

- Antibody-antigen interactions,
- Protein-protein interactions,
- Nucleic acid interactions,
- Enzyme interactions,
- Cellular interactions; microorganism, proteins,
- Interactions using biomimetic materials, synthetic bioreceptor, aptamers, peptides.

Raman Spectroscopy

- 1888-1970
- Discovered the inelastic scattering phenomenon in 1928
- Was awarded the Nobel Prize for Physics in 1930

Chandrasekhara Venkata Raman

When radiation passes through a transparent medium, the species present scatter a fraction of the beam in all directions.

In 1928, the Indian physicist C. V. Raman discovered that the visible wavelength of a small fraction of the radiation scattered by certain molecules differs from that of the incident beam and furthermore that the shifts in wavelength depend upon the chemical structure of the molecules responsible for the scattering.

Raman Spectroscopy

- The theory of Raman scattering shows that the phenomenon results from the same type of quantized vibrational changes that are associated with infrared absorption. Thus, the difference in wavelength between the incident and scattered visible radiation corresponds to wavelengths in the mid-infrared region.
- The Raman scattering spectrum and infrared absorption spectrum for a given species often resemble one another quite closely.

THEORY OF RAMAN SPECTROSCOPY

Raman spectra are acquired by irradiating a sample with a powerful laser source of visible or near-infrared monochromatic radiation. During irradiation, the spectrum of the scattered radiation is measured at some angle (often 90 deg) with a suitable spectrometer. At the very most, the intensities of Raman lines are 0.001 % of the intensity of the source; as a consequence, their detection and measurement are somewhat more difficult than are infrared spectra.

Excitation of Raman Spectra

A Raman spectrum can be obtained by irradiating a sample of carbon tetrachloride with an intense beam of an argon ion laser having a wavelength of 488.0 nm (20492 cm^{-1}). The emitted radiation is of three types:

1. **Stokes** scattering
2. **Anti-stokes** scattering
3. **Rayleigh** scattering

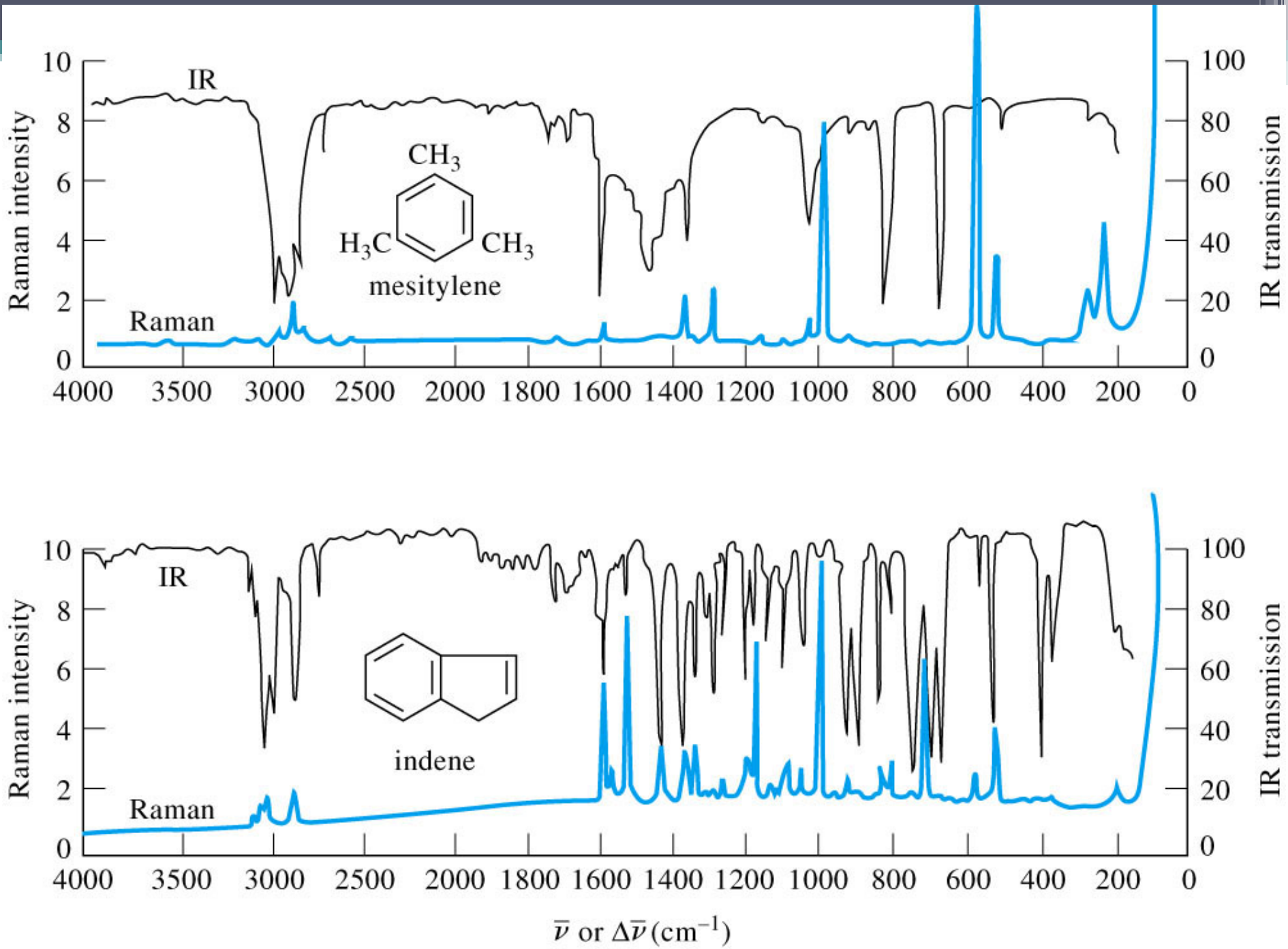

Applications of Raman Spectroscopy

- Raman Spectroscopy is a method of determining modes of molecular motions, especially vibrations. It is predominantly applicable to the qualitative and quantitative analyses of covalently bonded molecules.

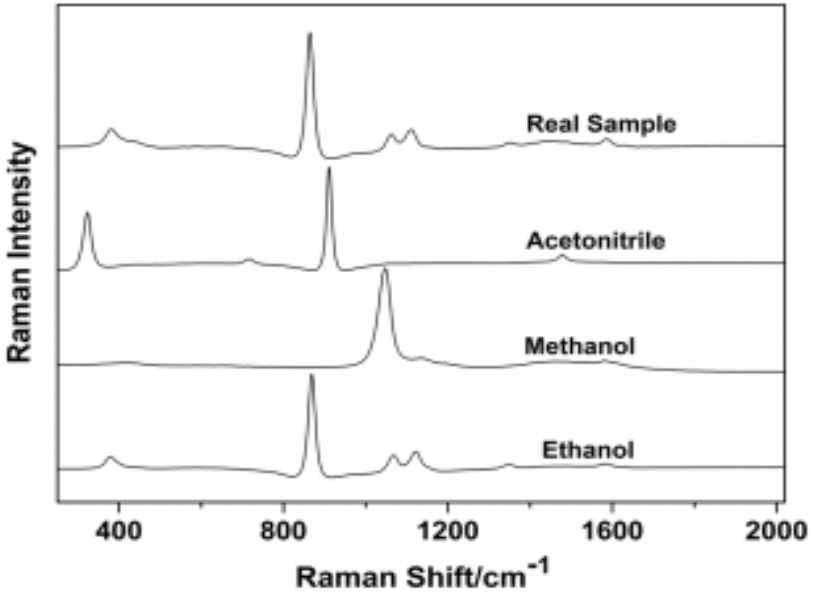

Figure 1. The Raman fingerprint spectrums of ethanol, methanol, acetonitrile, and a sample alcoholic beverage (gin).

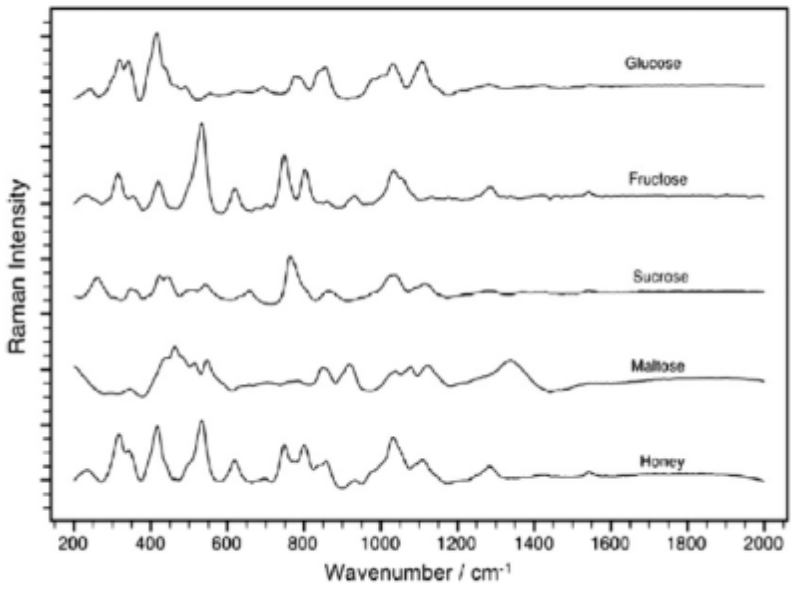

Fig. 1. The Raman spectra of glucose, fructose, sucrose, maltose and honey.

Surface Enhanced Raman Spectroscopy (SERS)

- SERS is a surface sensitive technique that results in the enhancement of Raman scattering by molecules adsorbed on rough metal surfaces.
- The enhancement factor can be as much as 10^{14} – 10^{15}, which allows the technique to be sensitive enough to detect single molecules.

Theoretical explanations for SERS

A. Electromagnetic field enhancement mechanism
   excitation of surface plasmon tends to form spacially localized “hot areas” the magnitude of enhancement ~10^6- 10^7 times for single colloidal silver, and ~10^8 for the gap between two coupled particles

B. Chemical enhancement
   due to specific interactions, forming charge-transfer complexes the magnitude of chemical enhancement ~10-100 times

SERS?

- High sensitivity
- Specificity
- Valuable tool for analyzing mixtures
- Low-power lasers and low magnification optics are suitable to acquire SERS spectra in very short acquisition times (typical ~10 s).
- Many applications—biochemistry, chemical manufacturing, environmental detection, forensics.

SERS application in bioassay
SERS reporter based application

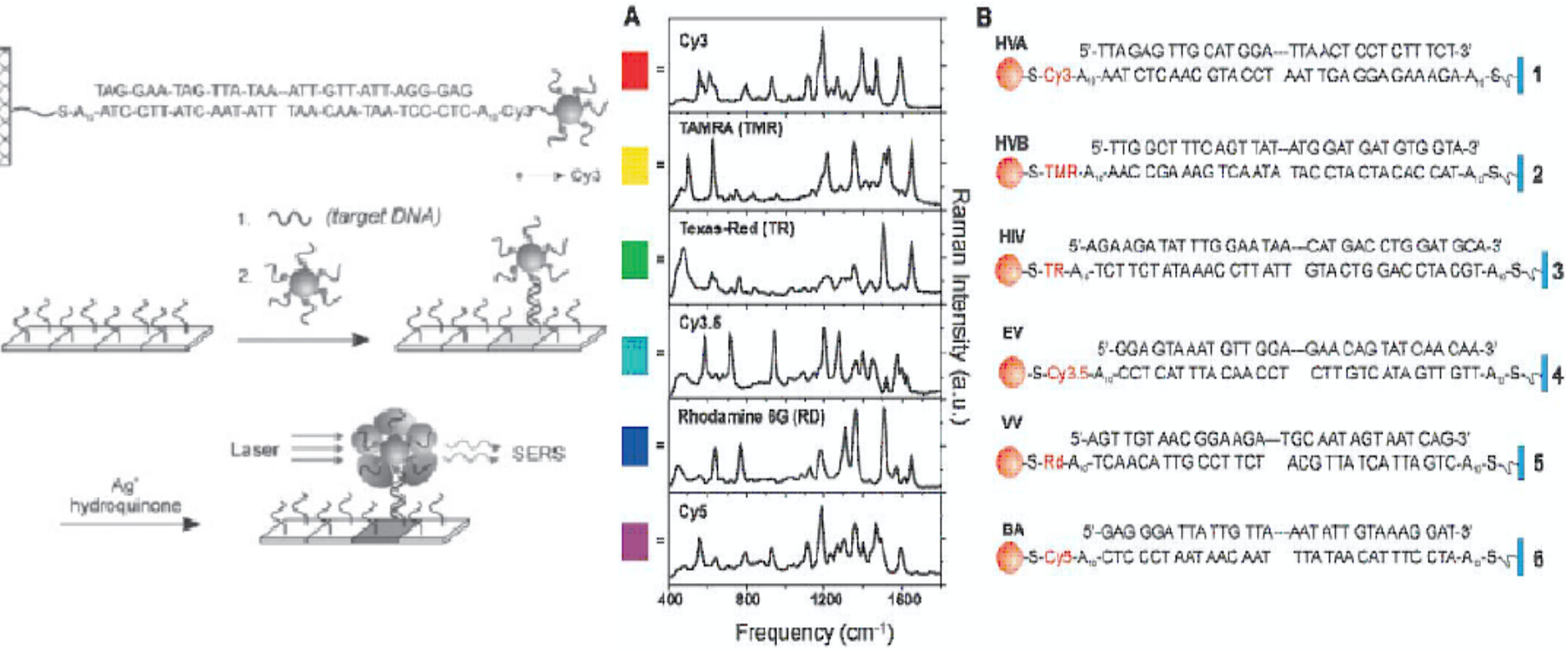

YunWei Charles Cao, Rongchao Jin, Chad A. Mirkin, Fingerprints for DNA and RNA Detection Nanoparticles with Raman Spectroscopic Science 297, 1536 (2002).

DNA Detection with Nanoprobes

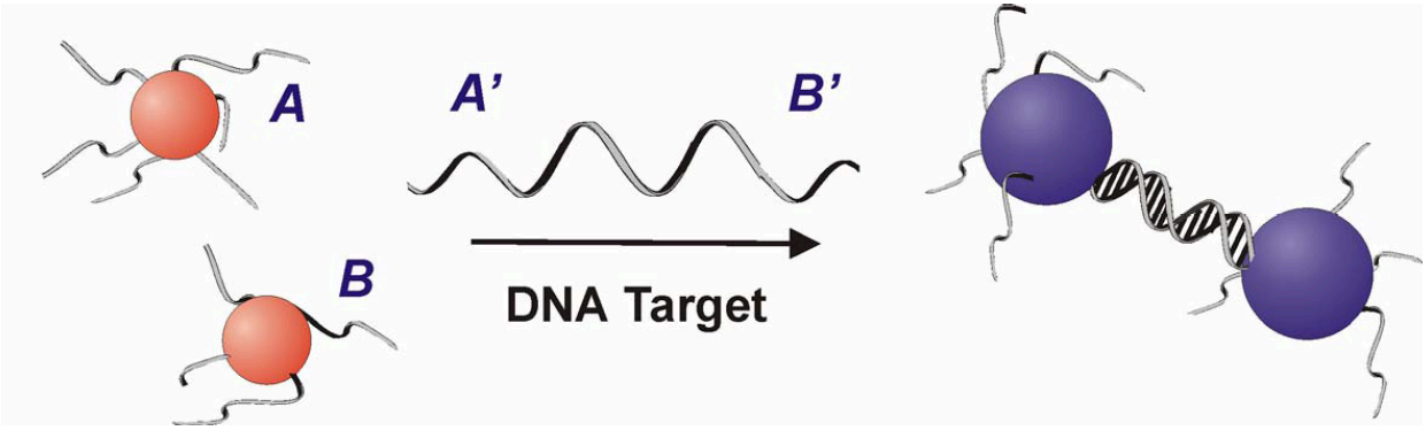

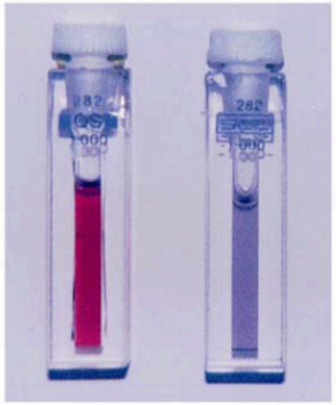

without target

with target

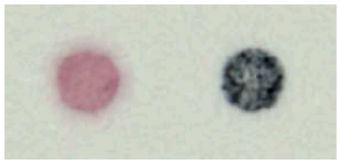

DNA Litmus Test

http://enhancinginnovation.wustl.edu/Mirkin.pdf

SERS application in bioassay

- SERS reporter based application

Advantages:

- SERS reporter gives a unique “fingerprint” signal
- enables ultrasensitive detection
- provides specific attachment to target biomarker
- minimizes biological interference
- Multiplexed detection of targets

Disadvantages:

- increase assay time,
- increase analyze steps

SERS application in bioassay

- **Label-free SERS detection**

  SERS offers the advantages of

  - reduced assay times,
  - simple handling,
  - lower reactant volumes compared to methods where the target molecules are labeled.

  However,

  - in a complex biological matrix, it would also be difficult to obtain reliable results with SERS.
  - it is difficult to detect low level of target concentration.

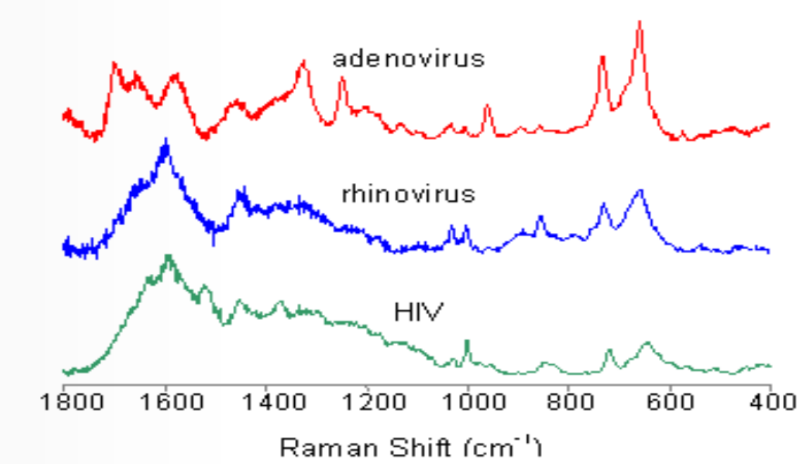

Fig. 2. SERS spectra of different virus
http://www.vet.uga.edu/ID/tripp/biosensing.php

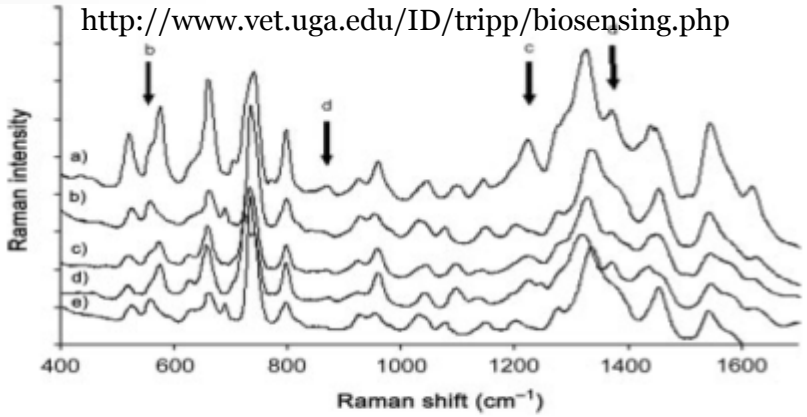

Figure 2. SERS spectra of the mixture of *S. sonnei*, *E. amylovara*, *P. vulgaris* and DH5α a), *S. sonnei* b), DH5α c), *E. amylovara* d) and *P. vulgaris* e). The arrows on the spectra of mixed bacterial sample indicate that they are from the bacterial spectra in mixtures that are distinguishable to the eye.

Culha M, Kahraman M, Cam D, Sayın I, Keseroglu K,
Surf. Interface Anal. 2010, *42*, 462–465

Food Components and Additives

- Proteins, peptides and amino acids
- Carbohydrayes
- Food lipids
- Enzymes
- Aroma and volatile compounds
- Vitamins
- Carotenoids and chlorophyll
- Flavanoids
- Food allergens and genetically modified componer

RESEARCH/ FOOD QUALITY

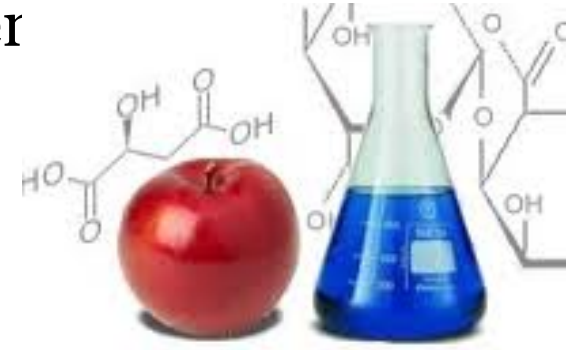

Food Contaminants

- Pesticide residues
- Pollutants
- Radioactive contaminants
- Pathogens and toxins

FOOD SAFETY

Neden mikroorganizma tayini önemlidir?

- Halk sağlığı
- Çevre sağlığı
- Gıda güvenliği
- Biyogüvenlik
- Biyoterör ajanı

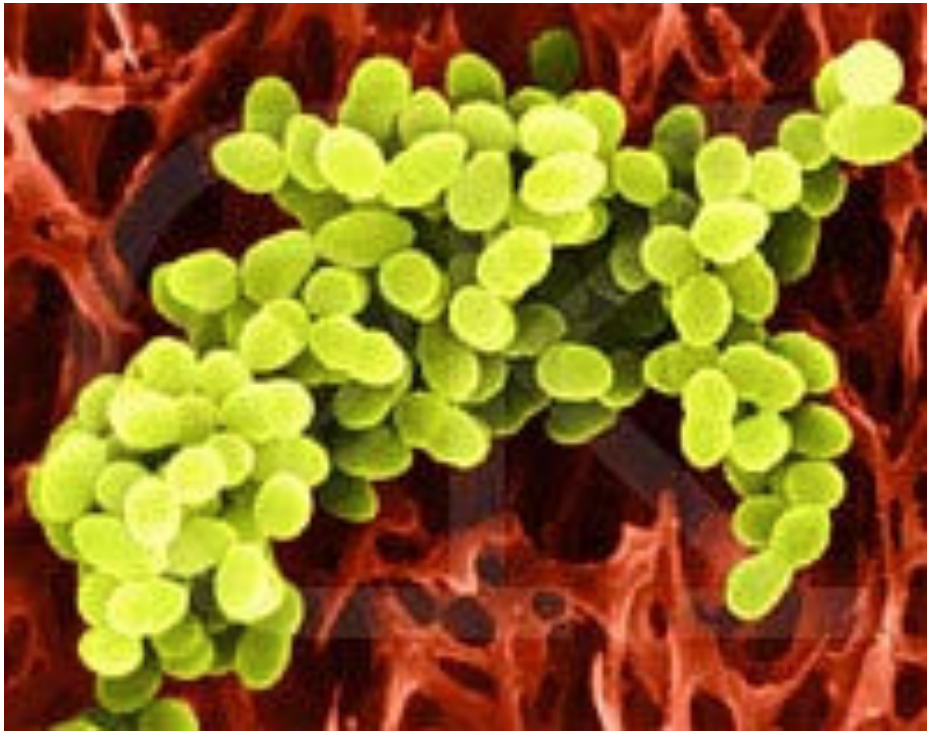

Staphylococcus aureus

If You Cannot Measure It, You Cannot Manage It!

Ölçemediğini yönetemezsin!

Mikroorganizma tayini yöntemleri

- Kültürel yöntemler
- Mikroskobik yöntemler
- Kimyasal yöntemler
- Fiziksel yöntemler
- Biyokimyasal yöntemler
- Moleküler yöntemler
- İmmünolojik yöntemler
- Biyosensörler


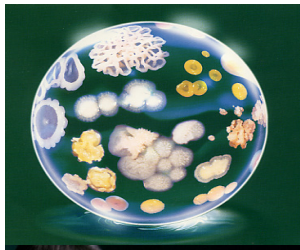

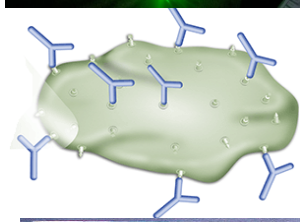
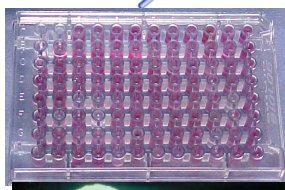
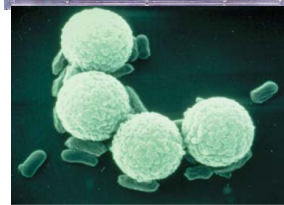

Kültürel yöntemler

- Seçici bir besiyerinde mikroorganizmaların yetişebilme kabiliyetini temel almaktadırlar
- Sadece canlı mikroorganizmalar saptanabilmektedir.
- Sıvı veya katı besiyerleri kullanılmaktadır
- Optik olarak mikroorganizmalar saptanmaktadır

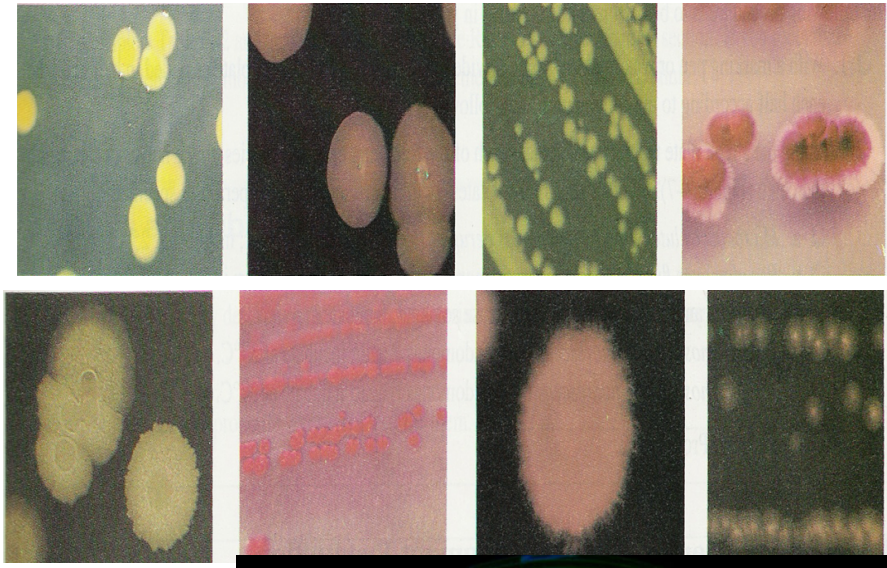

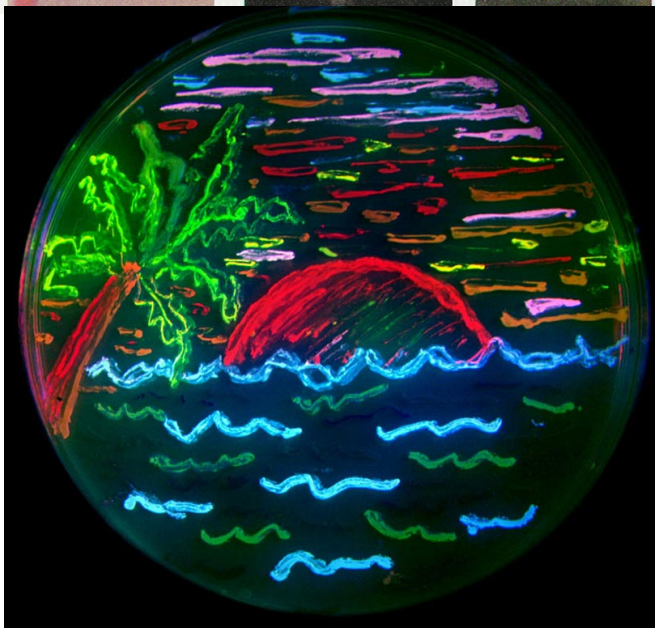

Kültürel yöntemler

- Uzun inkübasyon sürelerine gereksinim duyulmaktadır.
- Zahmetli yöntemlerdir.

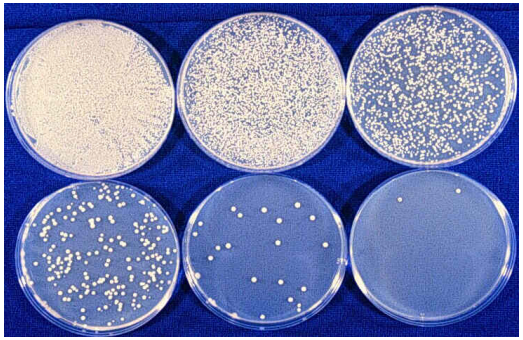

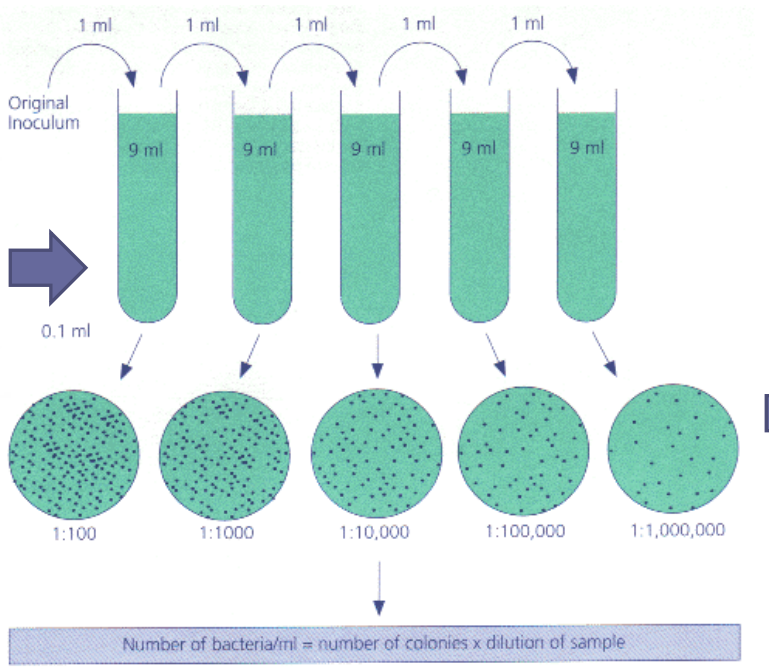

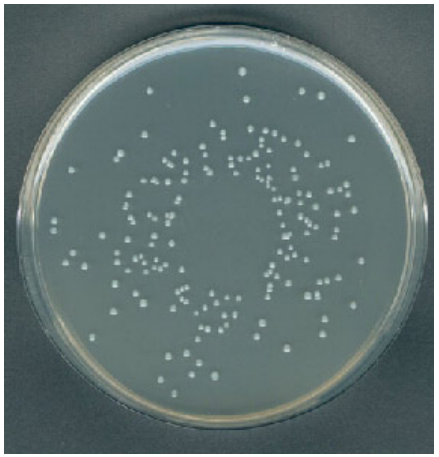

Analiz süresi 1-7 gün arasında değişmektedir.

Mikrobiyolojik analizlerde hızlı yöntemlere gereksinim duyulmaktadır.

HEDEF

100 ml içme suyu içerisindeki 1 *Escherichia coli*'nin saptanması.

Hızlı
Hassas
Seçici

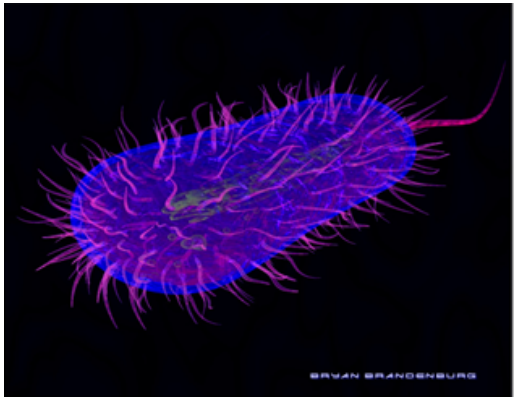

A sensitive detection platform based on surface-enhanced Raman scattering for *Escherichia coli* enumeration

The identification and quantification of microorganisms have become a key point in biodefense, food safety, diagnostics, and drug discovery research.

Identification of a microorganism is usually realized by traditional approaches such as culture-based and colony-counting methods which, in most cases, require several handling steps.

The traditional methods are time consuming and inconvenient. Hence, rapid identification and detection of pathogens are needed.

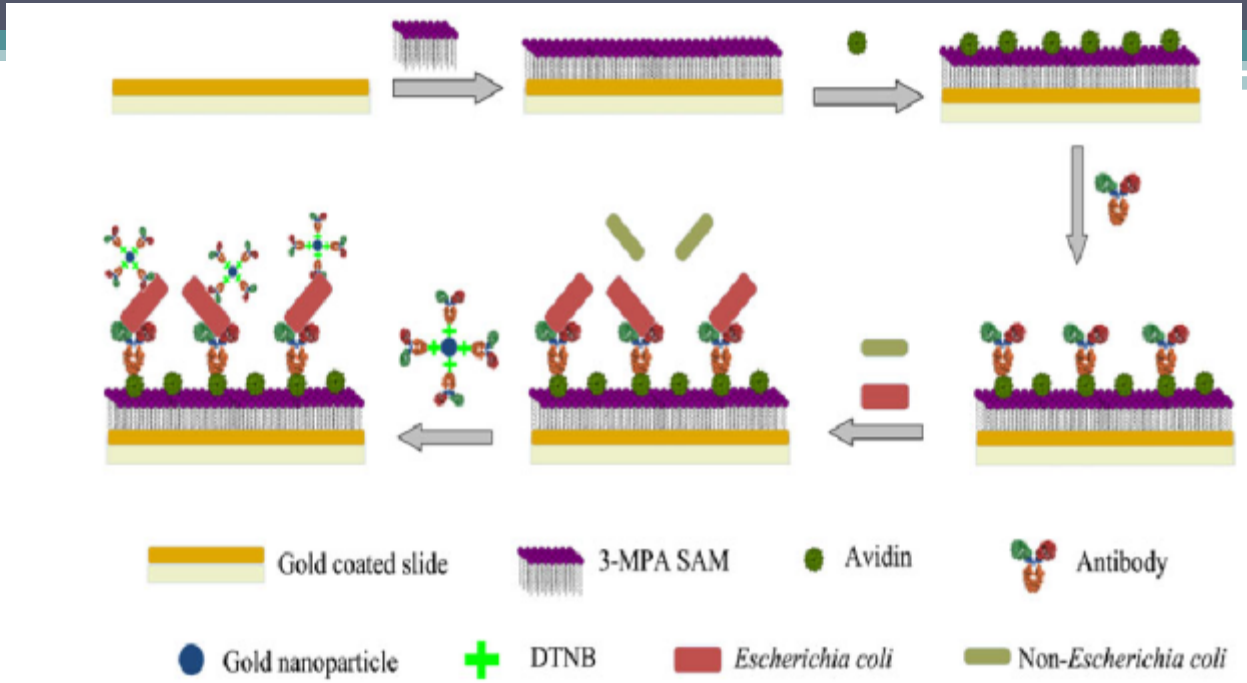

Scheme 1 Schematic of the SERS-based sandwich immunoassay for *E. coli* enumeration

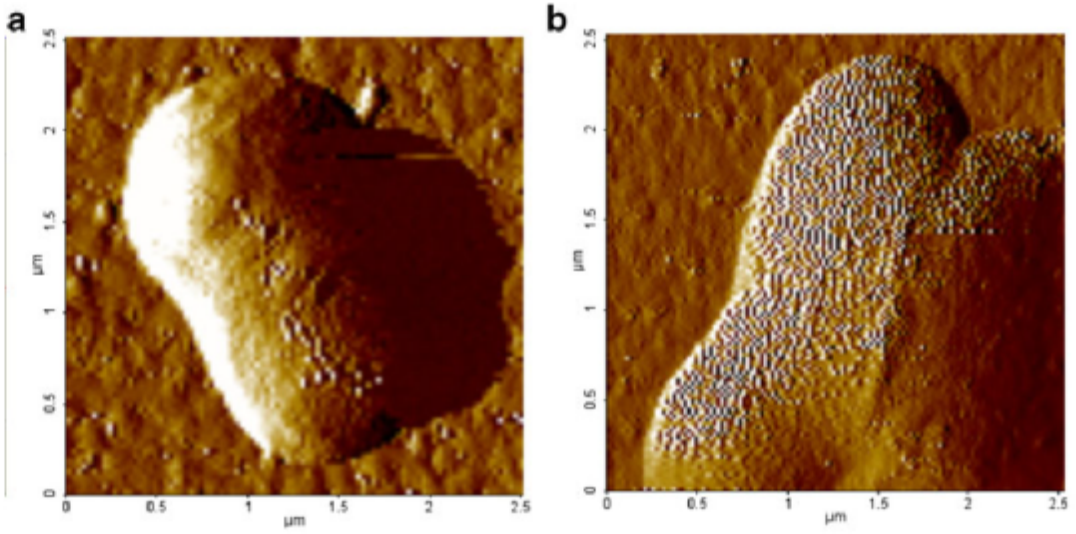

Fig. 4 AFM error images of **a** *E. coli*, **b** *E. coli* coated with gold nanorods, and **c** the 3D topography image of *E. coli* coated with spherical gold nanoparticles

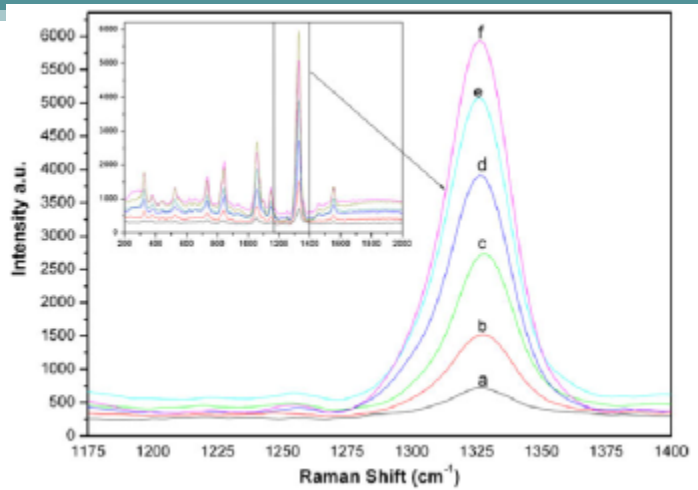

Fig. 5 Symmetric NO_2 stretching bands of DTNB at different *E. coli* concentrations obtained with spherical gold nanoparticles. **a** No *E coli*, **b** 10^1 cfu/mL, **c** 10^2cfu/mL, **d** 10^3 cfu/mL, **e** 10^4 cfu/mL, and **f** 10^5 cfu/mL

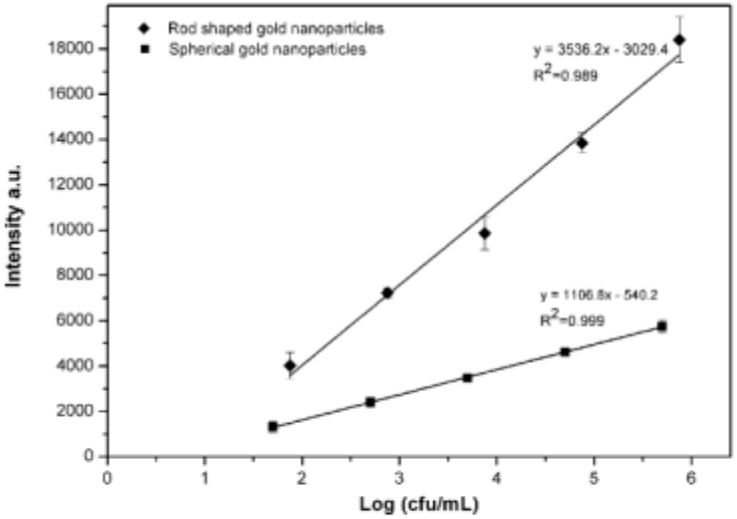

Fig. 7 Calibration curves for *E. coli* obtained at 10^1–10^5 cfu/mL by using spherical gold nanoparticles (■), and rod-shaped gold nanoparticles (♦)

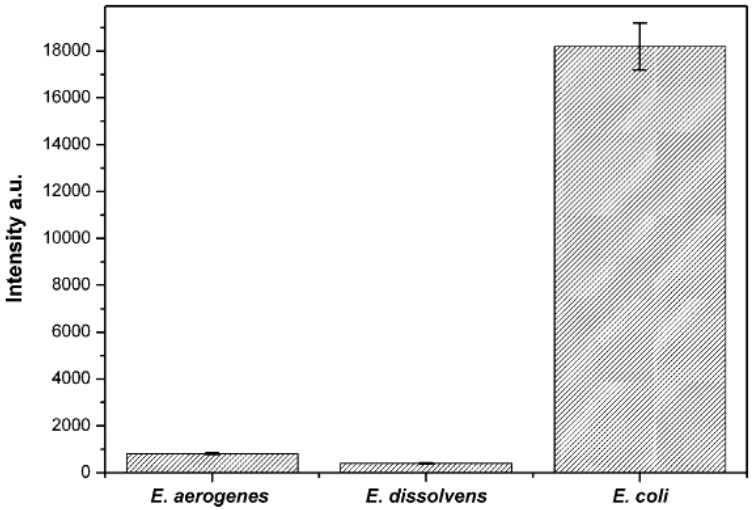

Fig. 8 The intensities measured for *E. aerogenes* (3.1×10^5 cfu/mL), *E. dissolvens* (4.3×10^5 cfu/mL), and *E. coli* (5.0×10^5 cfu/mL)

Temur et al., Anal Bioanal Chem (2010) 397:1595–1604

SERS-based sandwich immunoassay using antibody coated magneticnanoparticles for *Escherichia coli* enumeration

In this study, we have demonstrated that the magnetic properties of nanoparticles could be used to develop a reliable, sensitive and selective SERS-based homogeneous sandwich immunoassay. The magnetic spherical nanoparticles were prepared and *E. coli* capture efficiency of the nanoparticles was evaluated. Rod-shaped nanoparticles were used as a SERS reporter.

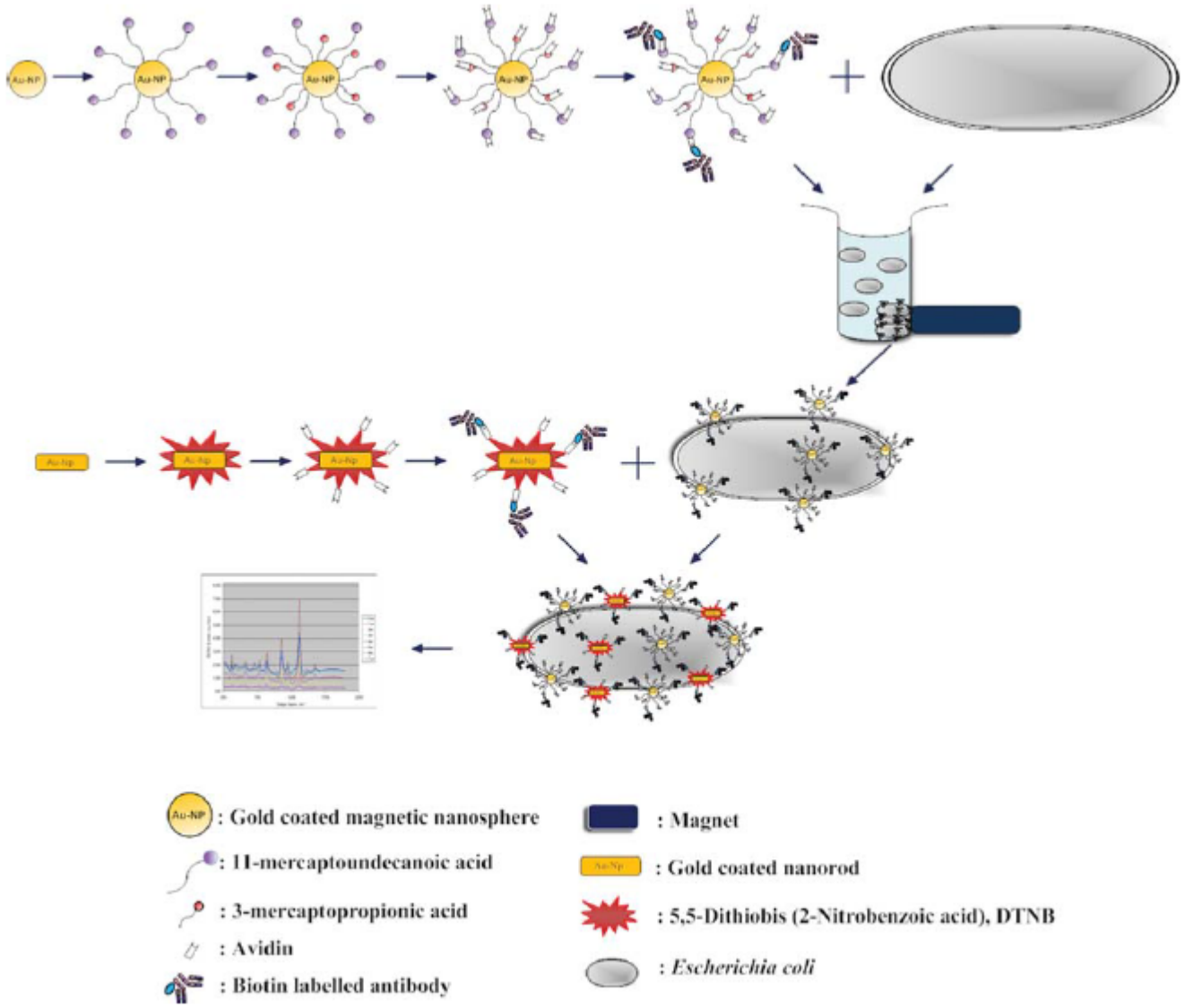

Fig. 1 Schematic illustration of IMS and SERS-based sandwich immunoassay for *E. coli* enumeration.

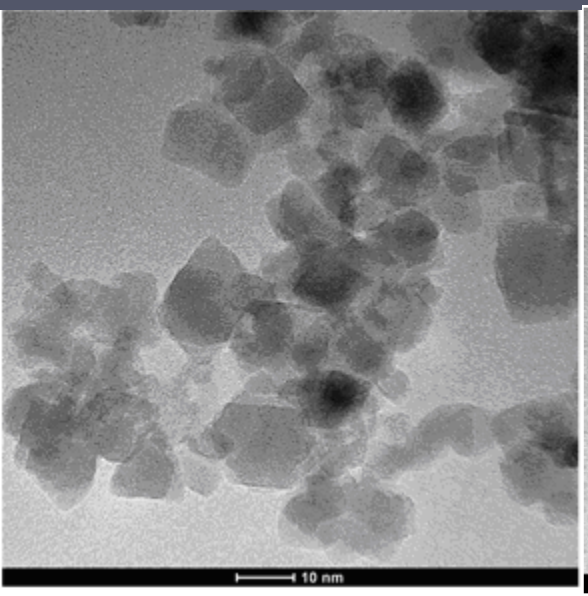

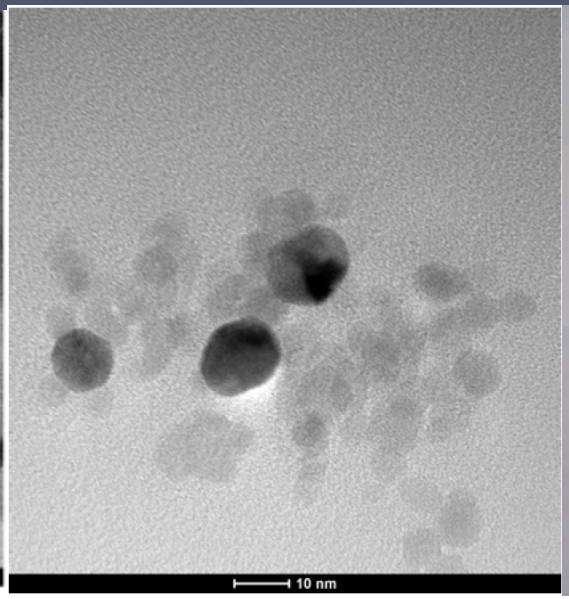

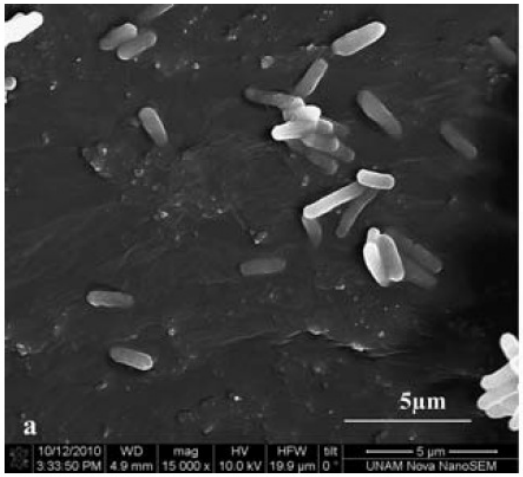

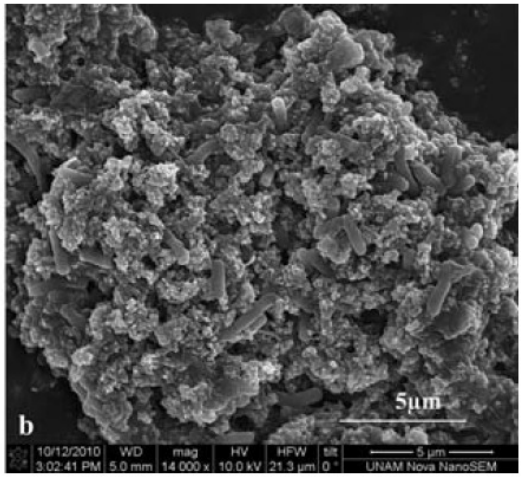

Fig. 6 Scanning electron micrograms of (a) control (*E. coli* without nanoparticle), (b) *E. coli*–Ab-coated nanoparticle–SERS reporter sandwich complex.

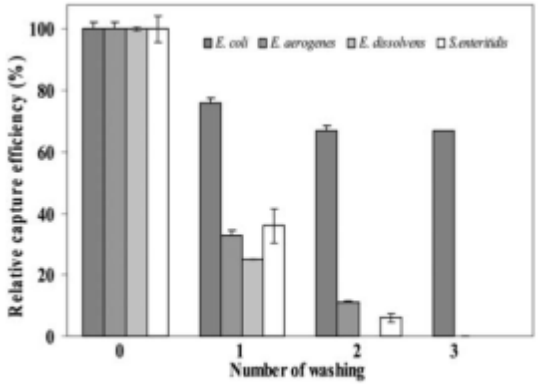

Fig. 3 Effect of number of washing stages on capture efficiency.

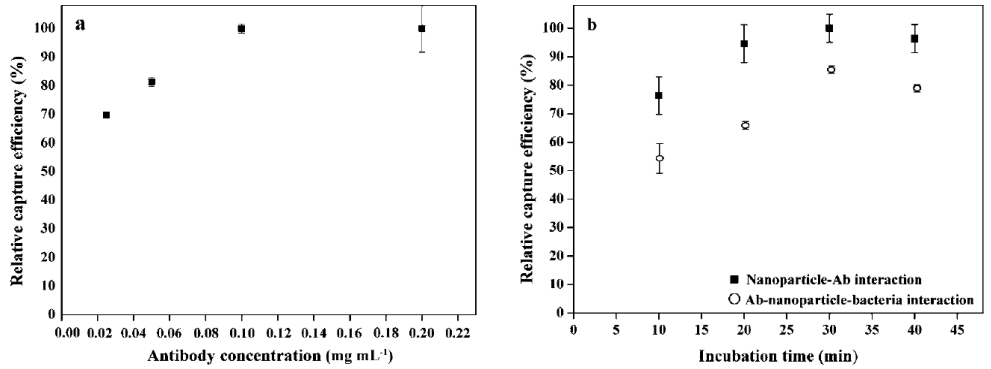

Fig. 4 Optimization of the parameters. (a) Effect of the Ab concentration on capture efficiency, (b) effect of the Ab–nanoparticle incubation time and Ab–nanoparticle–bacteria incubation time on capture efficiency.

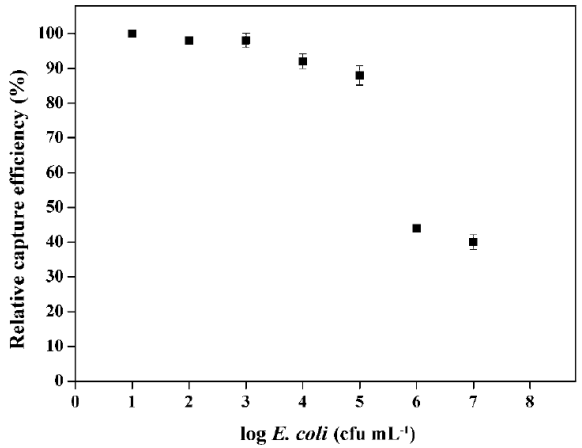

Fig. 5 Capture efficiency of nanoparticles with different concentrations of *E. coli* (10^1–10^7 cfu mL^{-1}).

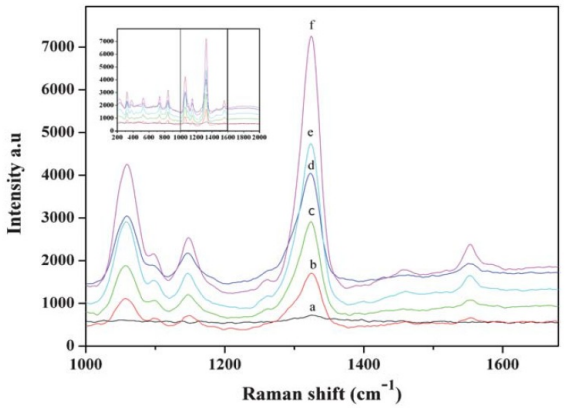

Fig. 7 Symmetric NO_2 stretching bands of DTNB ranging from 10^1 to 10^5 cfu mL^{-1} *E. coli* concentration obtained with rod shaped nanoparticles (a) No-*E. coli*, (b) 4.7×10^1 cfu mL^{-1}, (c) 4.7×10^2 cfu mL^{-1} (d) 4.7×10^3 cfu mL^{-1}, (e) 4.7×10^4 cfu mL^{-1}, and (f) 4.7×10^5 cfu mL^{-1}

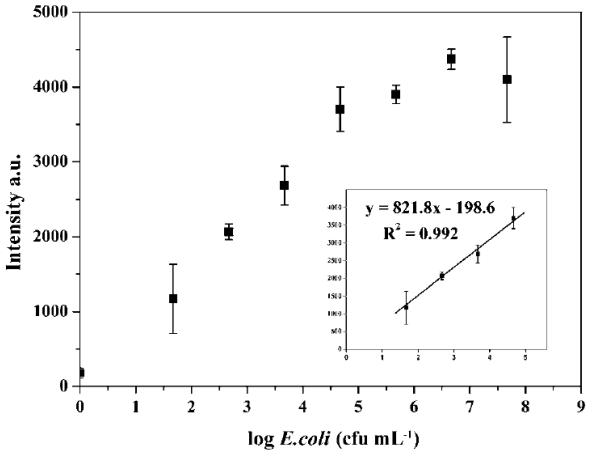

Fig. 8 Calibration curve for *E. coli* at a concentration range of 10^1–10^7 cfu mL^{-1} obtained by using gold nanoparticles.

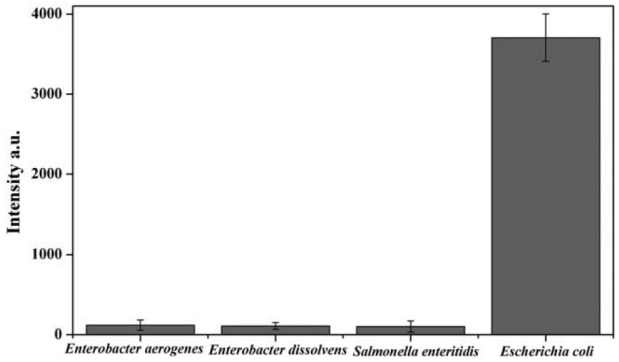

Fig. 9 The intensities measured for *E. aerogenes* (6.6×10^4 cfu mL^{-1}), *E. dissolvens* (4.7×10^4 cfu mL^{-1}), *S. enteriditis* (1.67×10^4 cfu mL^{-1}), and *E. coli* (1.7×10^4 cfu mL^{-1}).

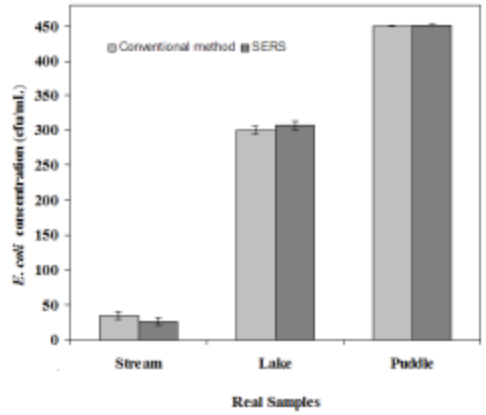

RESULTS

- In this study, we developed a rapid, sensitive, and selective immunoassay for the enumeration of *E. coli* in water samples using SERS.
- The developed immunoassayhad a working range of $4.7\times\ 10^{1}$–4.7×10^{4} cfu mL^{-1} with a detection limit of 8 cfu mL^{-1}
- Total assay time of less than 70 min including capturing of bacteria (30 min), formation of sandwich complex (30 min) and SERS measurement (less than10 min).
- The time for the developed method seems quite short when compared with other novel immunoassays.

A Rapid Method for Detection of Genetically Modified Organisms Based on Magnetic Separation and Surface-Enhanced Raman Scattering

- In this study, we have developed a new method for detection of genetic material using spherical magnetic gold nanoparticles and rod shaped gold nanoparticles.
- Rod shaped nanoparticles were used as a SERS reporter.
- The SERS signals were obtained and calibration curve was plotted to measure the different concentrations of target oligonucleotide.

- Optimum hybridization parameters were determined using high performance liquid chromatography.
- The selectivity and specificity tests of the developed assay were performed.
- Finally, this assay was applied to 35 S sequence of Bt-176 maize sample.
- The analytical performance of the SERS based sandwich assay system with respect to linear range, detection limit, response time, and selectivity was presented and discussed.

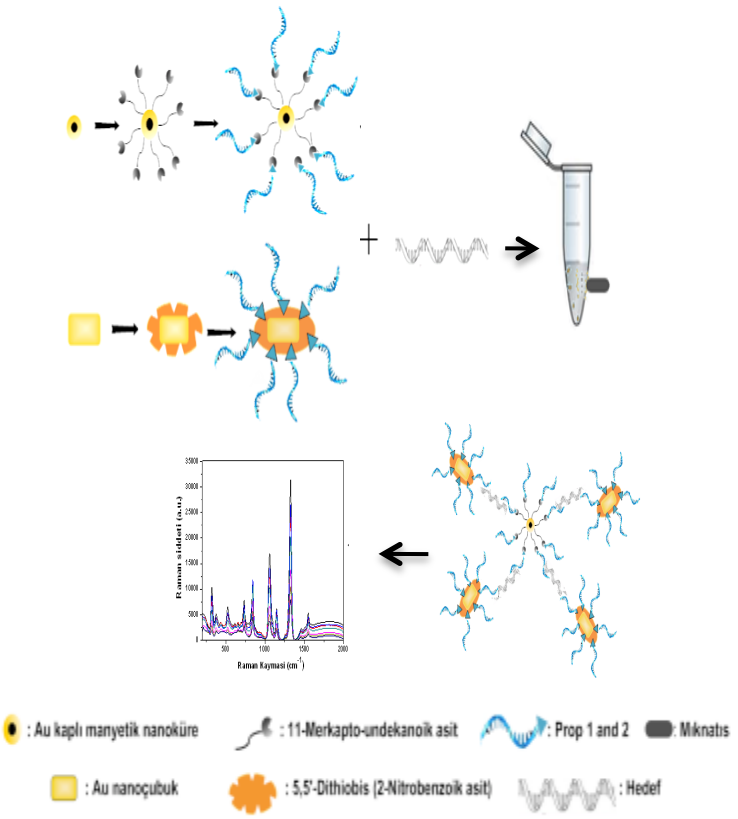

Fig. 1. Schematic illustration of MS-SERS based sandwich assay for target oligonucleotide.

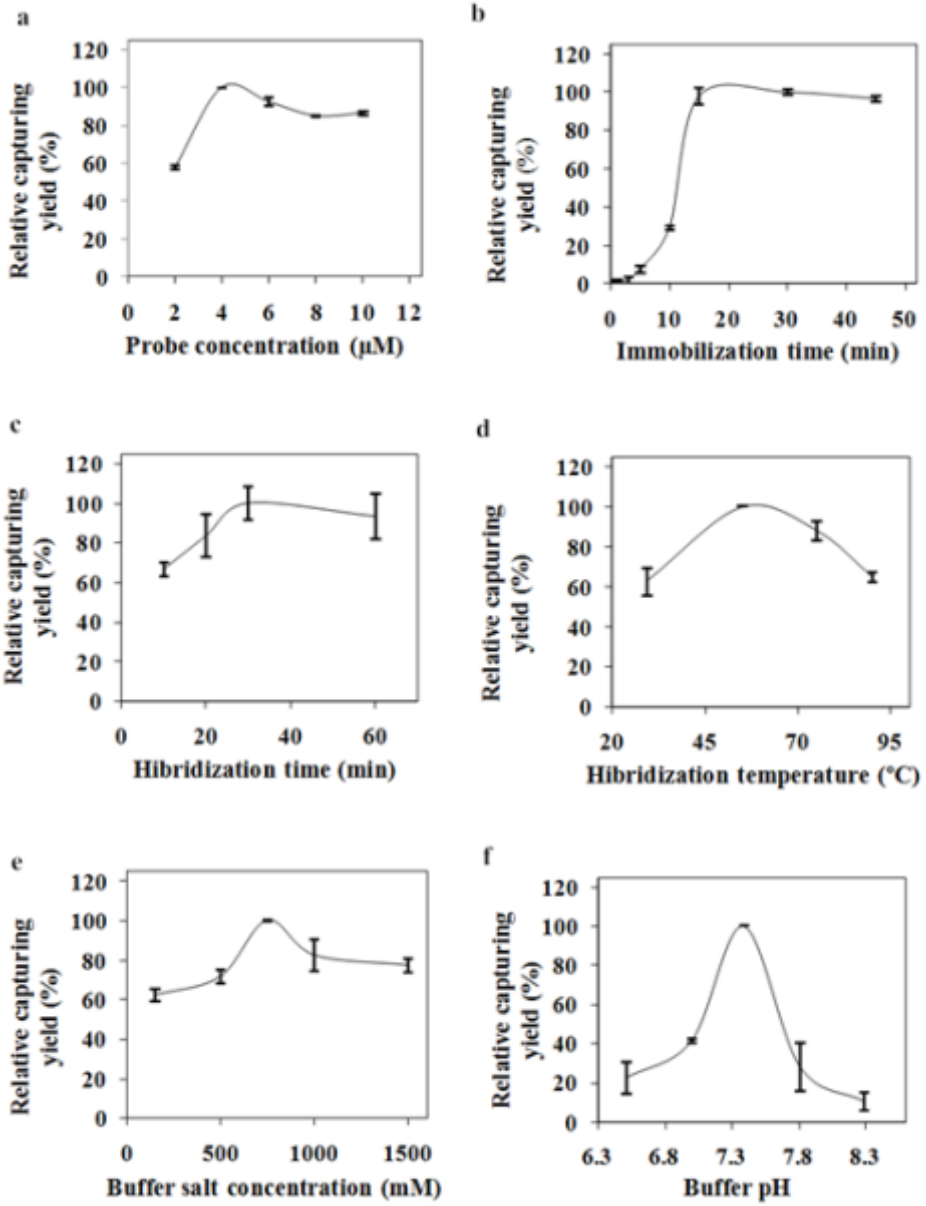

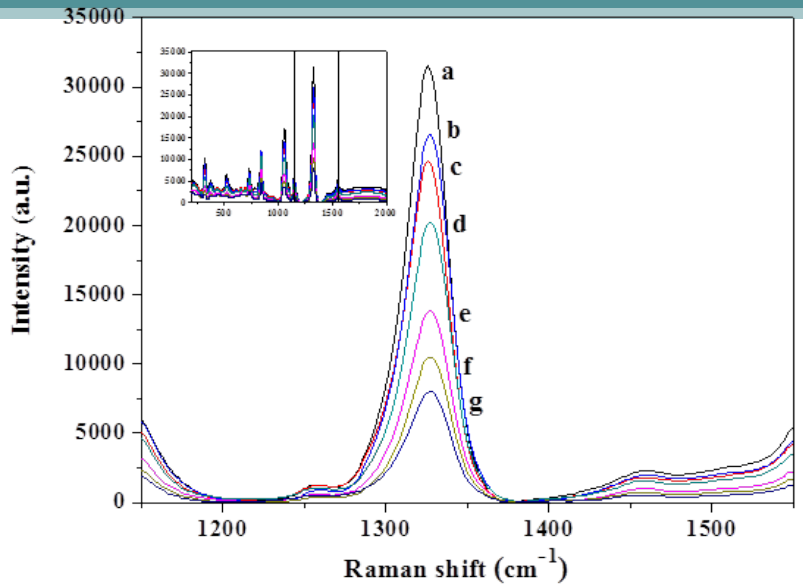

Fig. 3. Symmetric NO_2 stretching bands of DTNB range from 1000 nM to 0 nM target concentration obtained with rod shaped nanoparticles (a) 1000 nM, (b) 500 nM, (c) 100 nM, (d) 75 nM, (e) 50 nM, (f) 25 nM (g) 0 nM target concentration.

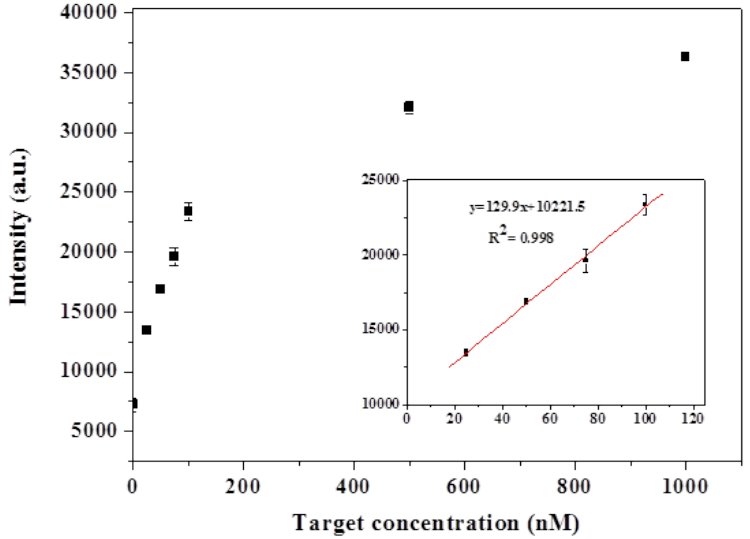

Fig. 4. Calibration curve for target oligonucleotide in range of 0-1000 nM

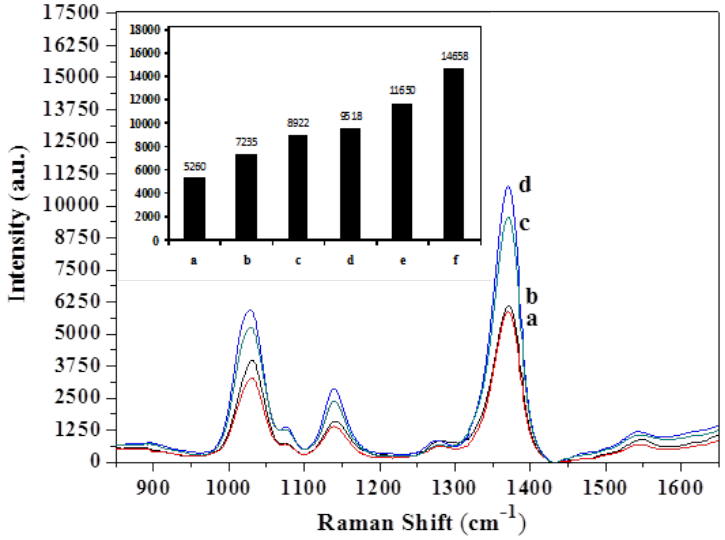

Fig. 5. Evaluation of specificity and selectivity of developed method (a) without probe 1, (b) without target, (c) without probe 2, (d) nonsense sequence, (e) intensity at LOD concentration, (f) intensity at LOQ concentration.

- The accuracy of the developed method was investigated with real sample (Bt-176 maize) genome

SERS method	Conventional method
28.2±4.3 nM	27.0±0.21 nM
91.8±5.4 nM	81.0±0.43 nM

Working range of developed assay is between 25 and 100 nM
Detection limit is 11 nM
Assay time is less than 40 min including in hybridization procedure (30 min) and SERS measurement (less than 10 min).

Detection of melamine in milk by surface-enhanced Raman spectroscopy coupled with magnetic and Raman labelled nanoparticles

- Melamine (1,3,5-triazine-2,4,6-triamine, $C_3H_6N_6$) is a chemical compound commonly used for the production of melamine resins
- Because of its high nitrogen content (66% by mass) melamine, was added to foods (milk, infant formula and pet food) as adulteration intentionally, to raise the apparent protein content
- Melamine adulteration along with the contaminant cyanuric acid (s-triazine-2,4,6-triol) has come into prominence because of the toxicity case in pets and infants
- In this study we investigated detecting melamine sensitively using SERS with magnetic sphere shaped nanoparticles and DTNB labelled rod shaped nanoparticles. The magnetic nanoparticles and DTNB labeled nanoparticles were connected to each other by the melamine molecule and constitute a complex structure. By the help of the magnetic nanoparticles, the composed complexed structure was sorted magnetically from the solution that contains free DTNB labelled nanoparticles. Obtained structure was analyzed by the Raman spectroscopy and the peak at 1366 cm^{-1} which is the most intense peak of DTNB, was pursued for melamine detection.

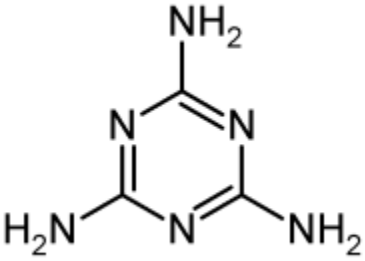

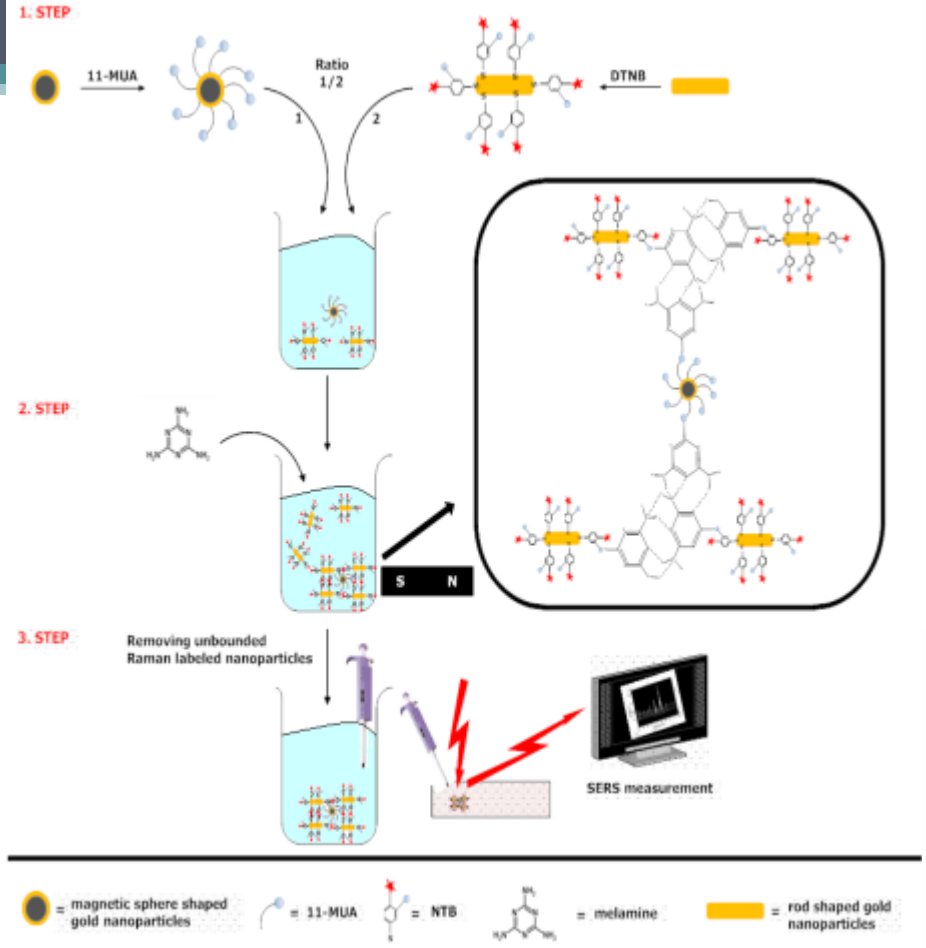

Fig. 1. Schematic illustration of melamine detection system preparation; 1. Step is preparation of nanoparticles for the melamine coupling: labelling rod shaped gold nanoparticle with DTNB, SAM constituting by 11-MUA on the magnetic sphere shaped gold nanoparticle surface and mixing these nanoparticles in ½ ratio (v/v), 2. Step is addition of melamine to the mixed nanoparticle solution the make a complex structure and separation of this structure magnetically from the unbounded nanoparticles, 3. Step is measurement of the SERS intensity.

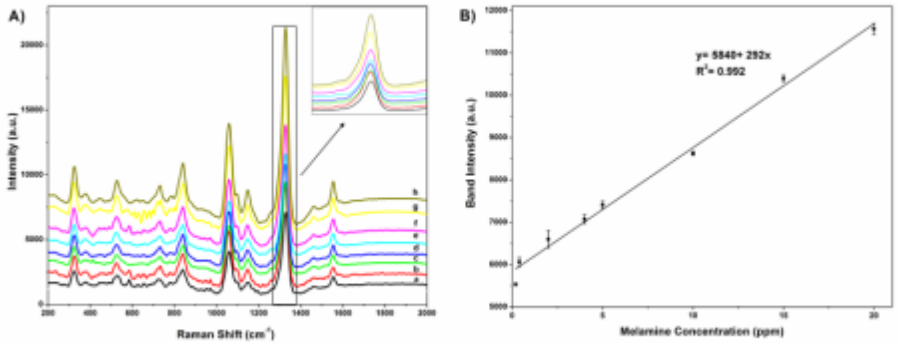

Fig. 2. (A) SERS spectra of melamine at different concentrations a) blank (phosphate buffer), b) 0.4 ppm, c) 2 ppm, d) 4 ppm, e) 5 ppm, f) 10 ppm, g) 15 ppm, h) 20 ppm. **(B)** Melamine concentration response curve in the range of 0.4-20 ppm of melamine concentration.

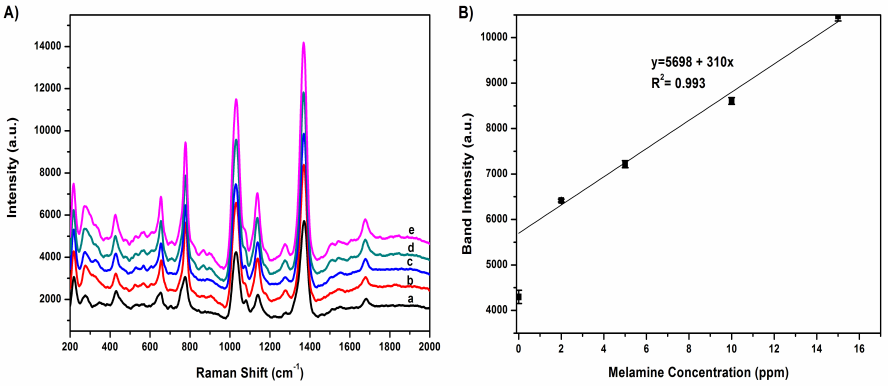

Fig. 3. (A) SERS spectra of spiked milk samples at different melamine concentrations a) blank, b) 2 ppm, c) 5 ppm, d) 10 ppm, e) 15 ppm. **(B)** Melamine concentration response curve of spiked milk samples in the range of 2-15 pmm of melamine concentration.

Spiked Concentrations of melamine (ppm)[a]	Average Peak Intensity (a.u.)	Amount Found[b] (ppm)	Recovery[c] (%) (n=6)	RSD (%)
blank	4297	-	-	-
2	6417	1.98	99	0.50
5	7217	4.72	94	1.07
10	8608	9.48	95	0.86
15	10477	15.78	105	1.07

Table 1 Recoveries for the analysed spiked milk samples.

[a] Spiked melamine in commercially obtained skim milk samples
[b] Average value of six determinations
[c] Recovery

Table 2 Inter-day and intra-day repeatability of the proposed method (Melamine concentration is 5 ppm).

Intra-day		Inter-day	
Measurements	Average band Intensity (a.u.)[a]	Days	Average band Intensity (a.u.)[a]
1	7320 (5.07)	1	7291 (4.97)
2	7271 (4.90)	2	7300 (5.00)
3	7309 (5.03)	3	7254 (4.84)
Average	7300 (5.00)		7282 (4.94)
SD[b]	20.7		19.9
RSD (%)[c]	0.28		0.27

[a] Average value of six determinations, corresponding melamine concentrations (ppm) are given in parenthesis
[b] Standard deviation
c Relative standard deviation (RSD (%) = (SD/mean) x 100)

- ✓ The LOD and LOQ were found as 0.35 ppm and 1.10 ppm, respectively. Similarly, for spiked milk samples, The LOD and LOQ was 0.31 ppm and 1.02 ppm, respectively.
- ✓ The safety limits melamine in dairy products is 1 ppm and 2.5 ppm for infants and adults, respectively.
- ✓ It can be seen that this method is sufficient enough to detect 1 ppm of melamine which is the important concentration level in infant food limitation.
- ✓ Assay time is less than 20 min including in incubation period (10 min) and SERS measurement (less than 10 min).

Attomole Sensitivity of Staphylococcal Enterotoxin B Detection Using an Aptamer-Modified Surface-Enhanced Raman Scattering Probe

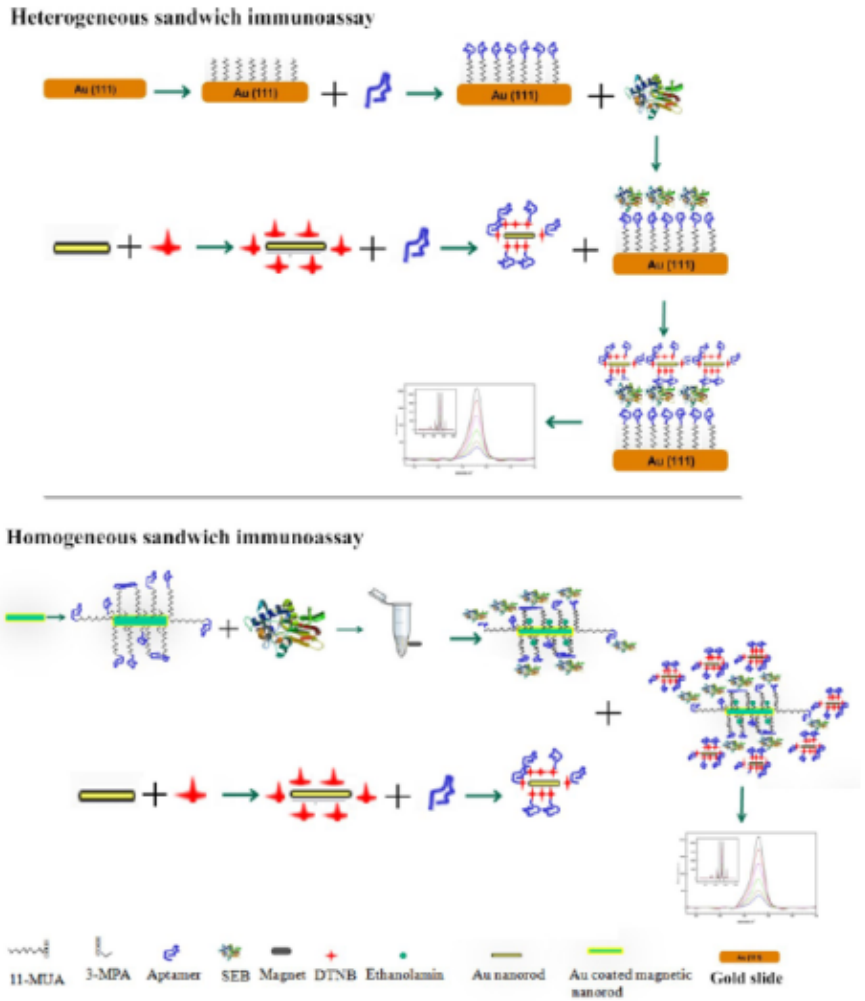

Figure 1. Schematic illustration of SERS-based heterogeneous and homogeneous sandwich immunoassay systems.

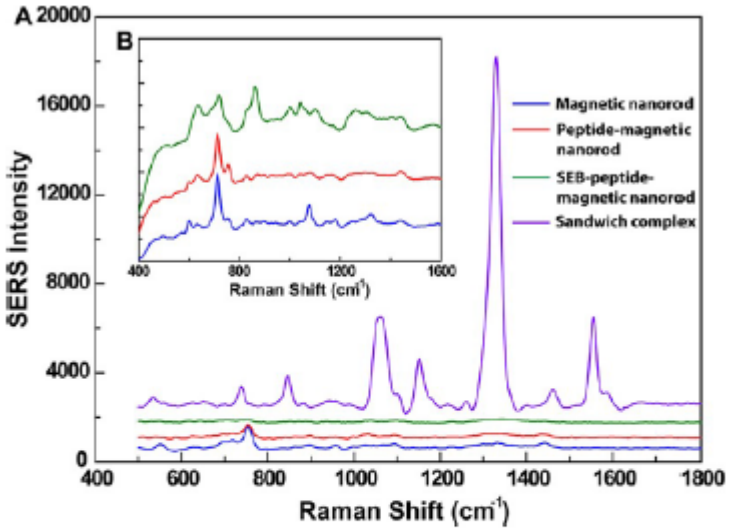

Figure 3. (A) SERS spectra of magnetic gold nanorods, peptide-immobilized magnetic gold nanorods, SEB-captured magnetic gold nanorods, and the sandwich complex of DTNB-labeled gold nanorod–SEB–peptide–magnetic gold nanorod. (B) SERS spectra of magnetic gold nanorods, peptide-immobilized magnetic gold nanorods, and SEB-captured magnetic gold nanorods obtained by adding silver nanoparticles.

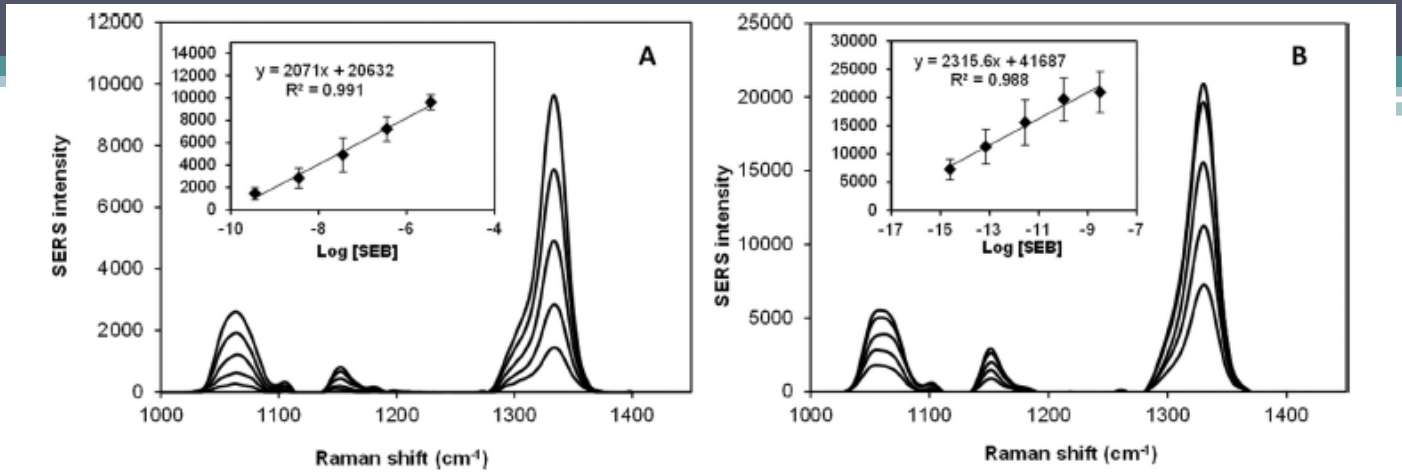

Figure 4. (A) SERS spectra of the sandwich complex at different SEB concentrations of 0, 3.5×10^{-10}, 3.5×10^{-9}, 3.5×10^{-8}, 3.5×10^{-7}, and 3.5×10^{-6} mol L^{-1} (from bottom to top) and the plot of the peak height of the DTNB SERS band 1338 cm^{-1} against the log[SEB] obtained by using gold slides. (B) SERS spectra of the sandwich complex at different SEB concentrations of 0, 2.5×10^{-15}, 7.0×10^{-14}, 2.8×10^{-12}, 1.1×10^{-10}, and 3.1×10^{-9} mol L^{-1} (from bottom to top) and the plot of the peak height of the DTNB SERS band 1338 cm^{-1} against the log[SEB] obtained by using magnetic gold nanorods.

The limit of detection (LOD), which corresponds to signal-to-noise ratio of 3, is 2.2 × 10–16 M (ca. 2697 SEB molecule/20 μL) for nanoparticle-based assay.

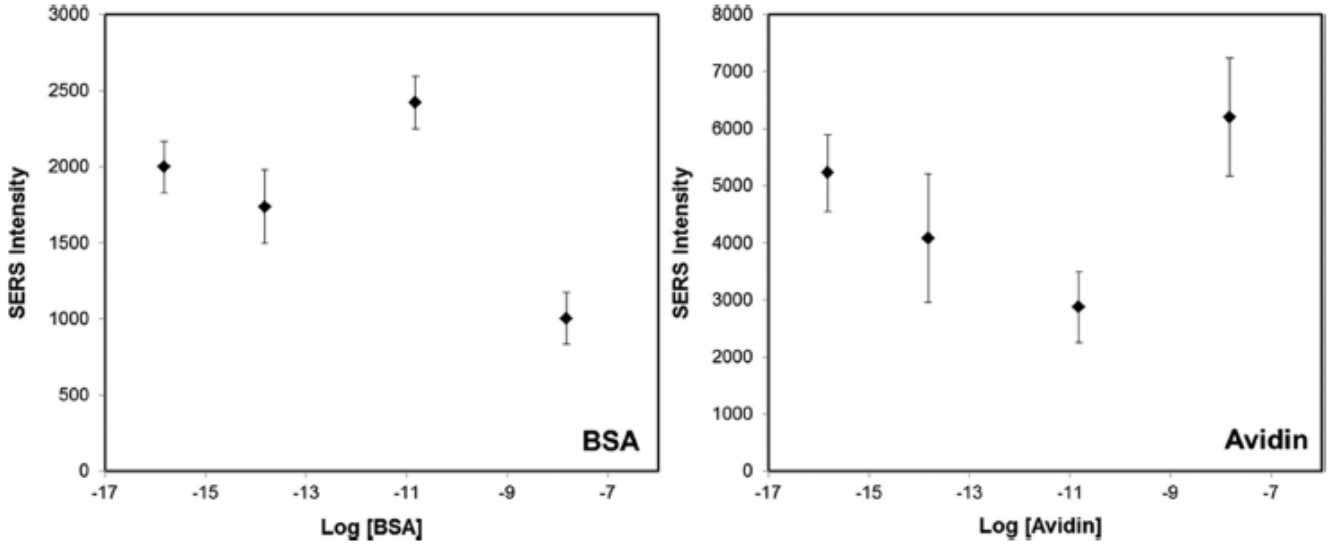

Figure 6. Plot of the peak height of the DTNB SERS band at 1338 cm^{-1} against log[BSA] and log[avidin] obtained by the developed method using magnetic gold nanorods.

Gold-Coated Iron Composite Nanospheres Targeted the Detection of *Escherichia coli*

Int. J. Mol. Sci. **2013**, *1*

Scheme 1. Schematic illustration of the surface modification of magnetic gold nanoparticles and *E. coli* assay.

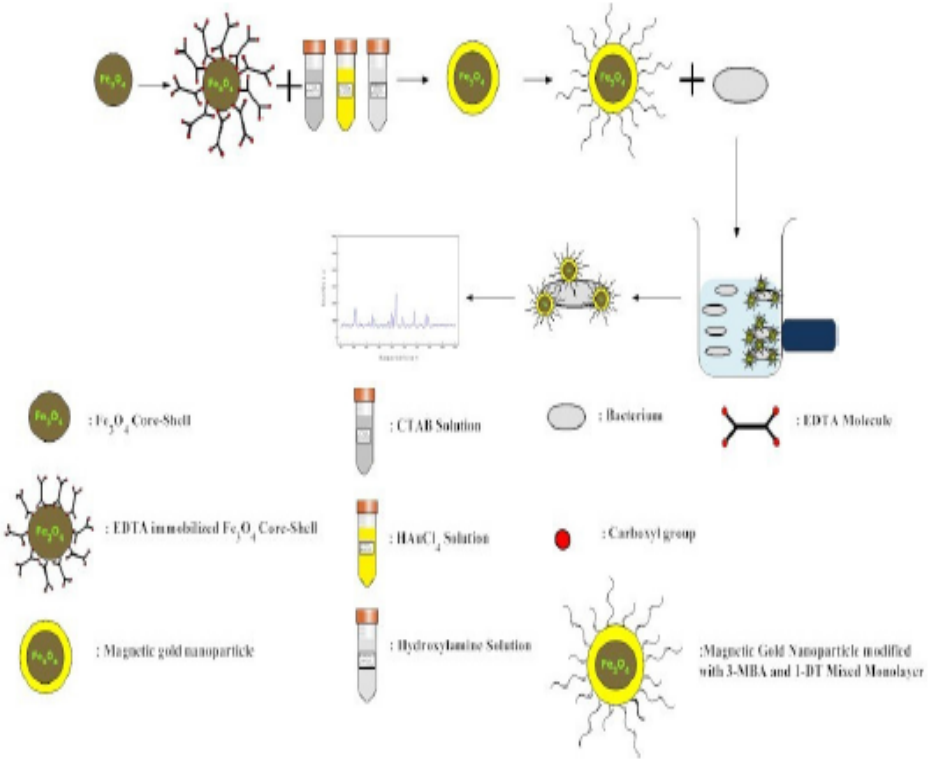

Figure 4. The scanning electron microscopy (SEM) images of *E. coli* immobilized with 3-MBA/1-DT modified magnetic nanoparticles on *E. coli*. Inset: The SEM image of unmodified *E. coli*.

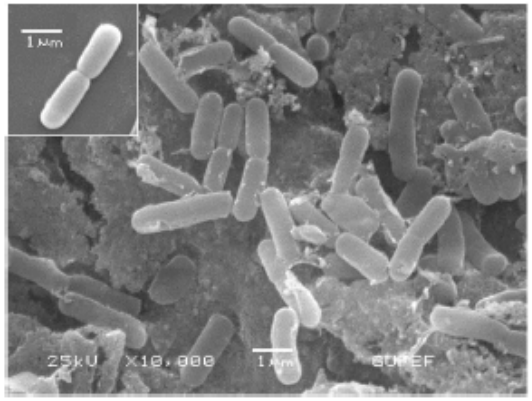

Figure 5. The SEM images of *E. coli* immobilized with (**A**) 3–MBA; (**B**) 1–DT; (**C**) CTAB– modified magnetic nanoparticles.

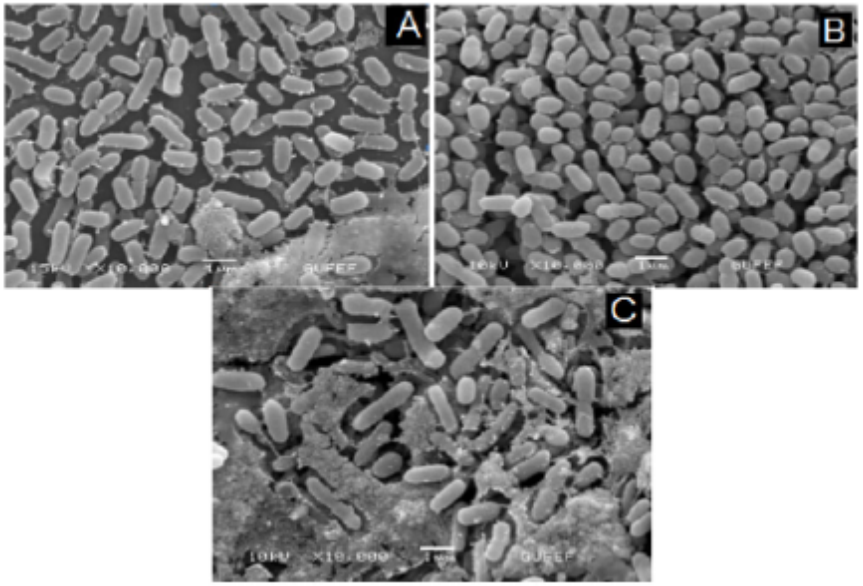

Figure 6. TEM image of *E. coli* immobilized with 3-MBA/1-DT modified magnetic nanoparticles

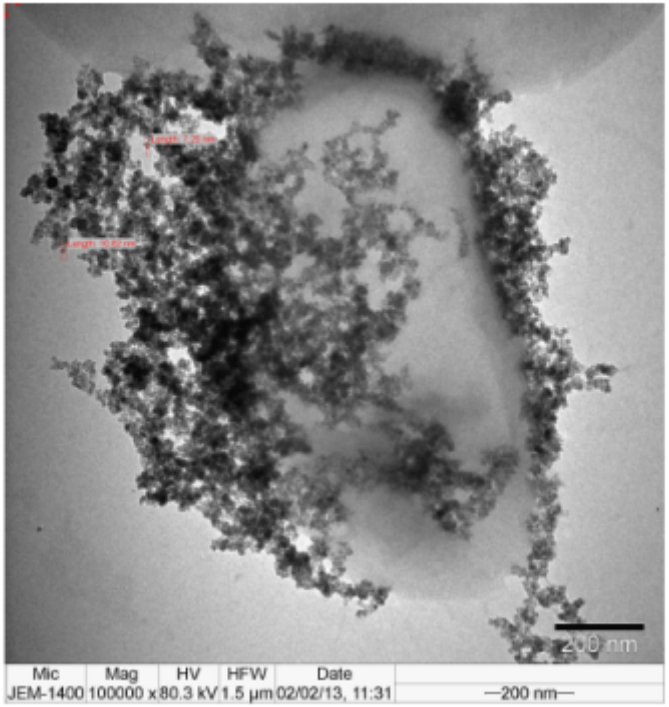

Figure 7. Surface-enhanced Raman scattering (SERS) spectrum of (**a**) 10^7 cfu mL^{-1} *E. coli*; (**b**) *E. coli* interacted with 3-MBA/1-DT-modified magnetic nanoparticles; (**c**) bacterial growth solution interacted with 3-MBA/1-DT-modified magnetic nanoparticles.

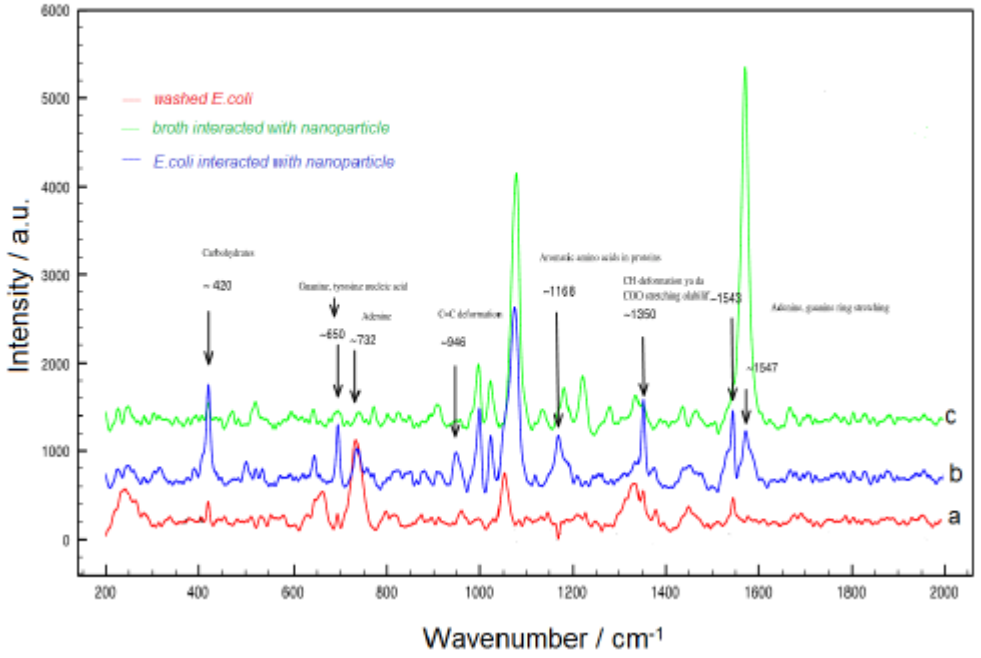

A novel approach for heavy metal detection based on surface enhanced Raman spectroscopy: Use of 1,8-naphthalimide modified poly(propylene amine) dendrimer as ligand

Interaction between four newly synthesised poly(propylene amine) dendrimers from first and second generations modified with 1,8-naphthalimide units and five important metal ions (Al^{3+}, Sb^{2+}, As^{2+}, Cd^{2+} and Pb^{2+}) were investigated by using surface-enhanced Raman spectroscopy (SERS). Principal component analysis was employed to discriminate the groups of these metal ions, which were interacted with each of the dendrimer molecules, separately.

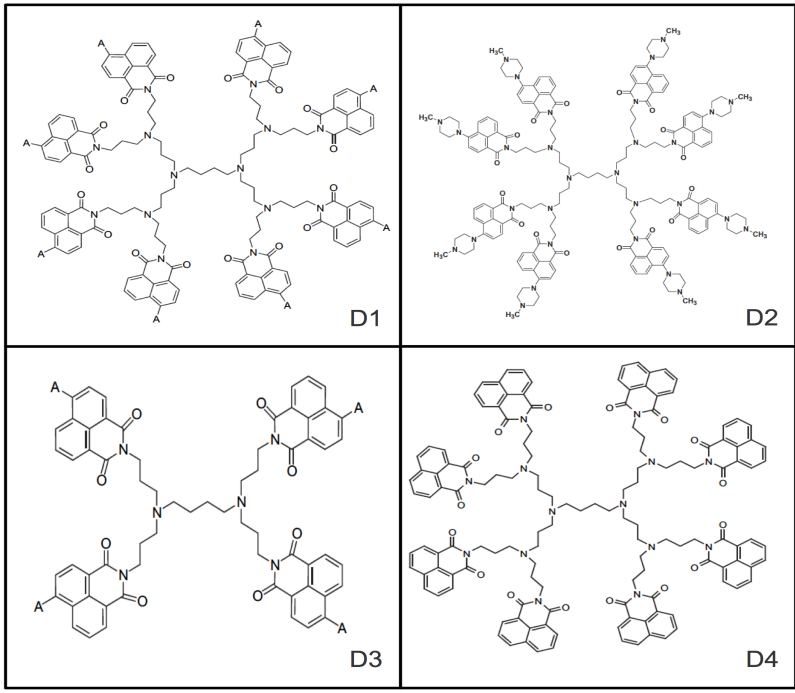

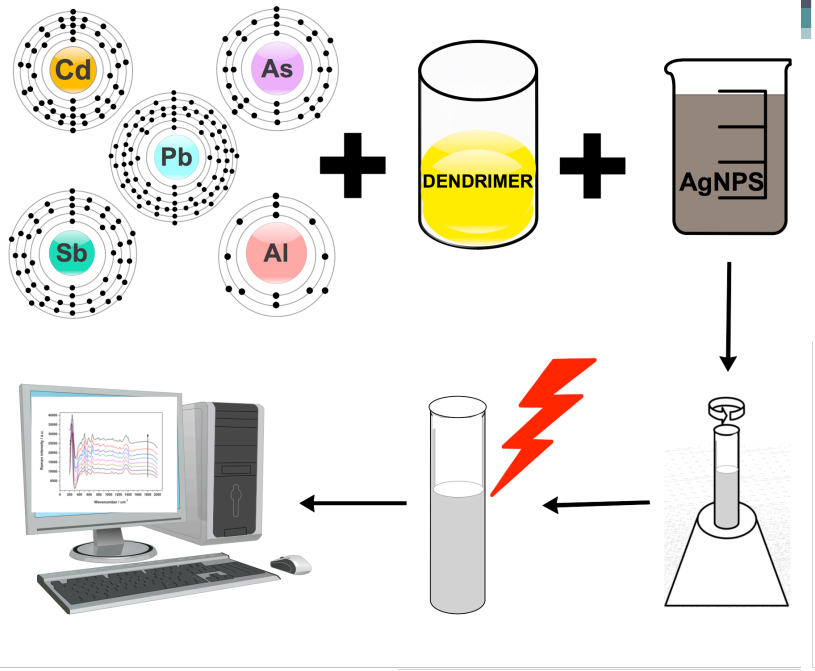
Cd
As
Pb
Sb
Al
DENDRIMER
AgNPS

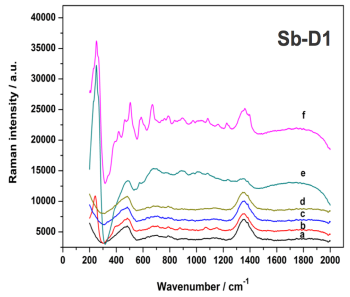
Sb-D1
Raman intensity / a.u.
Wavenumber / cm-1

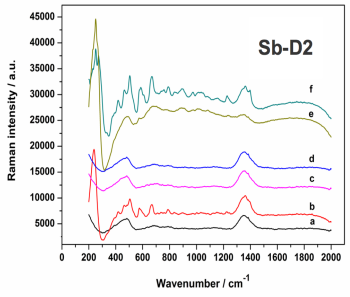
Sb-D2
Raman intensity / a.u.
Wavenumber / cm-1

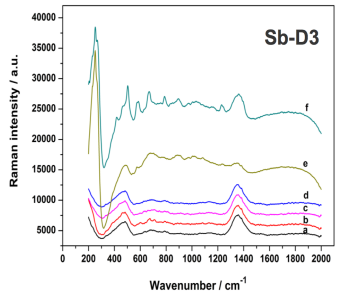
Sb-D3
Raman intensity / a.u.
Wavenumber / cm-1

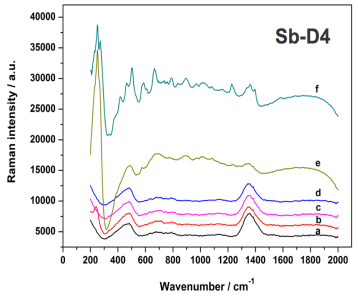
Sb-D4
Raman intensity / a.u.
Wavenumber / cm-1

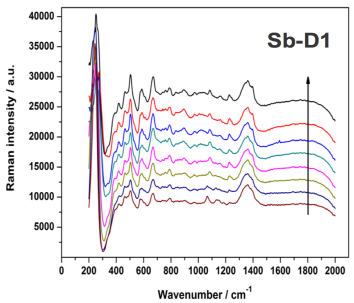
Sb-D1
Raman intensity / a.u.
Wavenumber / cm-1

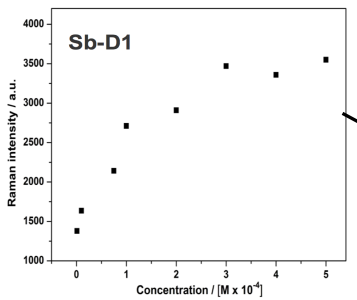
Sb-D1
Raman intensity / a.u.
Concentration / [M x 10-4]

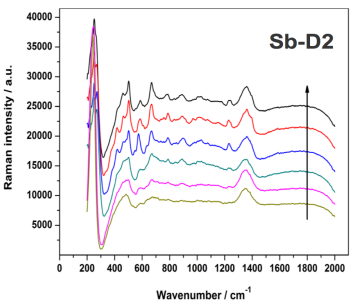
Sb-D2
Raman intensity / a.u.
Wavenumber / cm-1

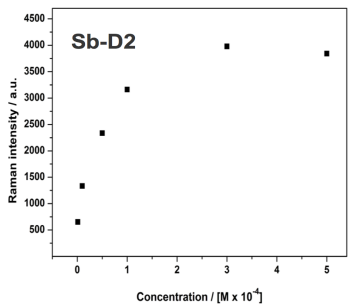
Sb-D2
Raman intensity / a.u.
Concentration / [M x 10-4]

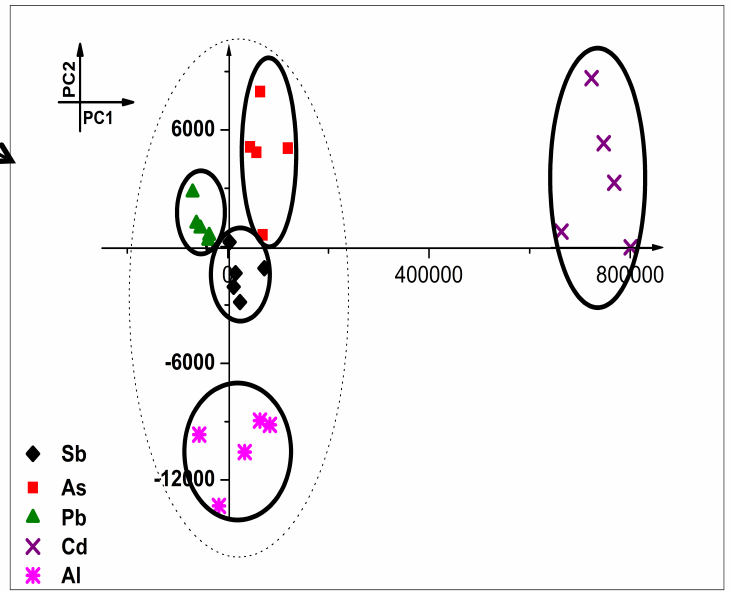
PC2
PC1
6000
-6000
-12000
400000
800000
Sb
As
Pb
Cd
Al

- Calibration curves were established for all metal ions between the concentration ranges of $5x10^{-4}$ to $1x10^{-6}$ M.
- It has been shown that these dendrimers can be coordinated, especially with different metal ions.
- Using dendrimer molecules and silver colloids at the same time allowed us to obtain an SERS signal from the abovementioned metal ions at very low concentrations.
- Four different PCA models were developed to accomplish the discrimination of five metal ions which interacted with each of the four dendrimer molecules separately.
- Assay time is less than 1 min.

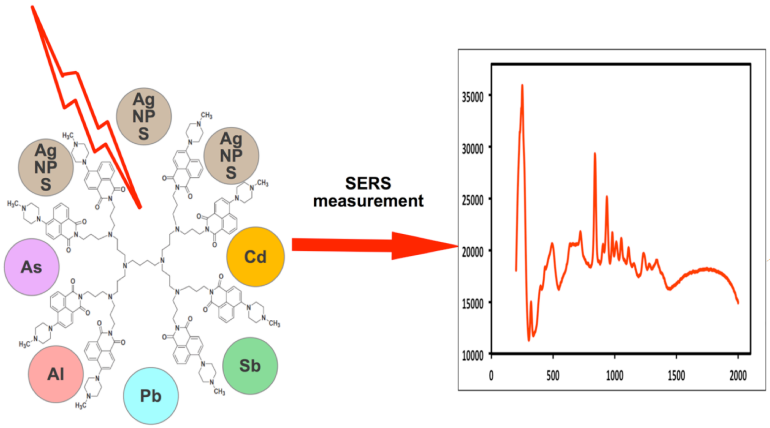

Fructose determination based on surface–enhanced Raman spectroscopy (SERS)

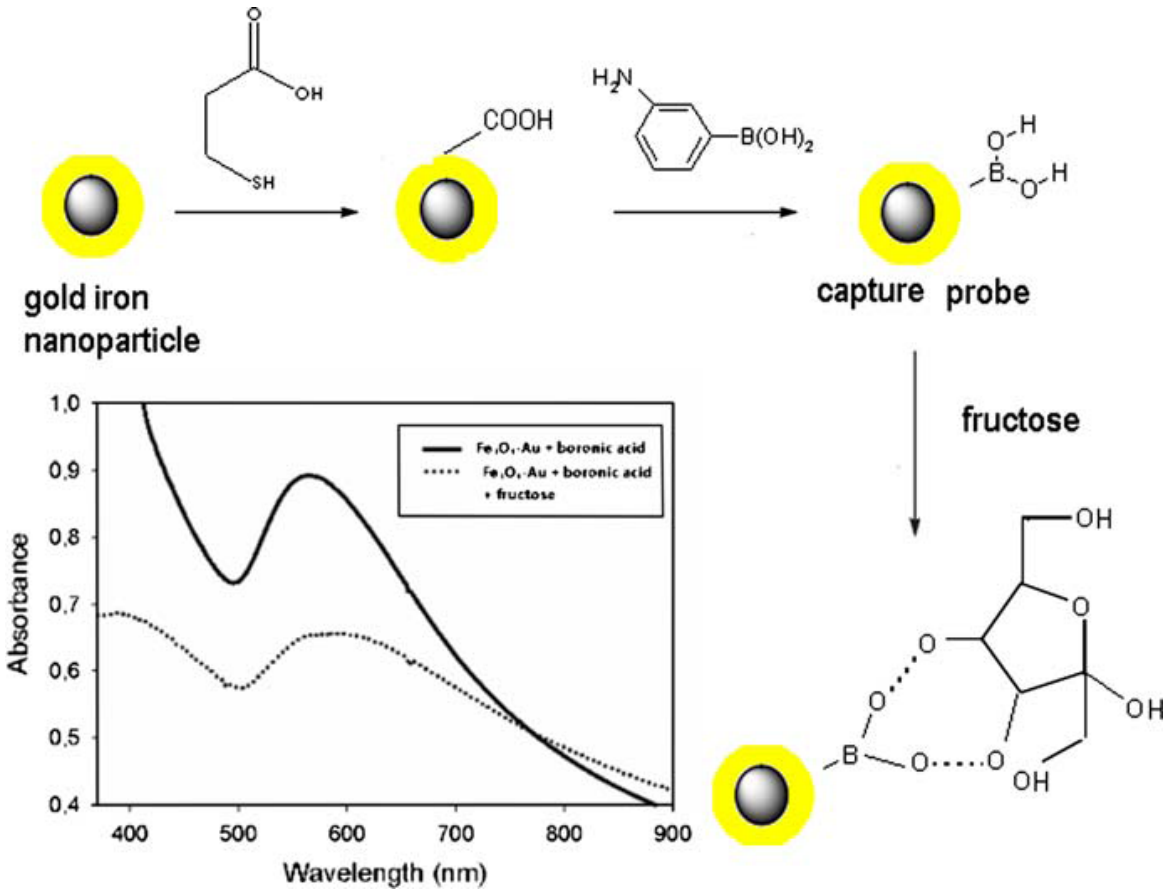

Schematic illustration of the functionalized nanoparticles formation process and UV–Vis spectra of boronic acid-modified Fe_3O_4–Au nanoparticles after interaction of the 3-aminophenylboronic acid-modified gold iron nanoparticle with fructose

Quantum dots

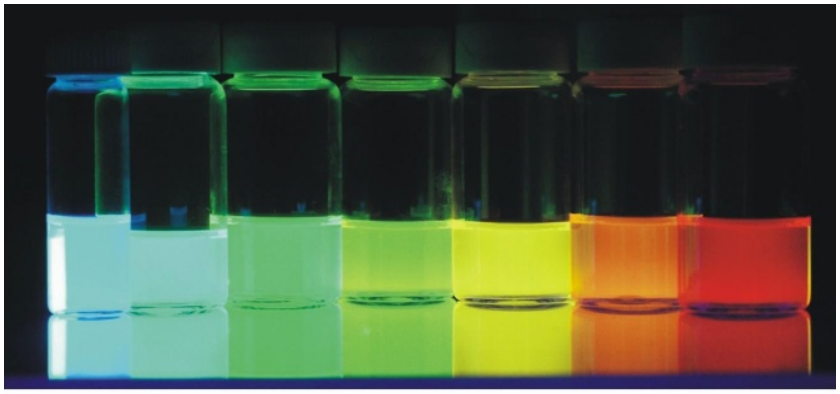

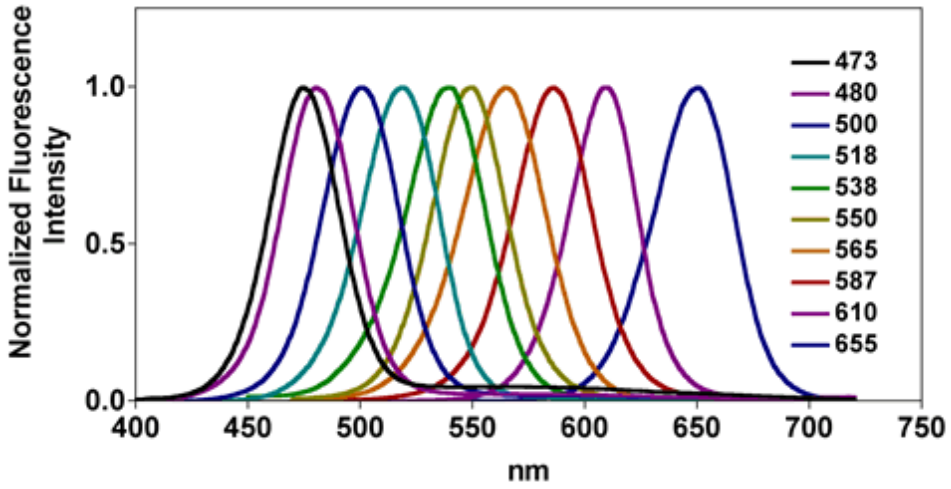

1. *Antibody was labelled with quantum dots for bacteria detection*

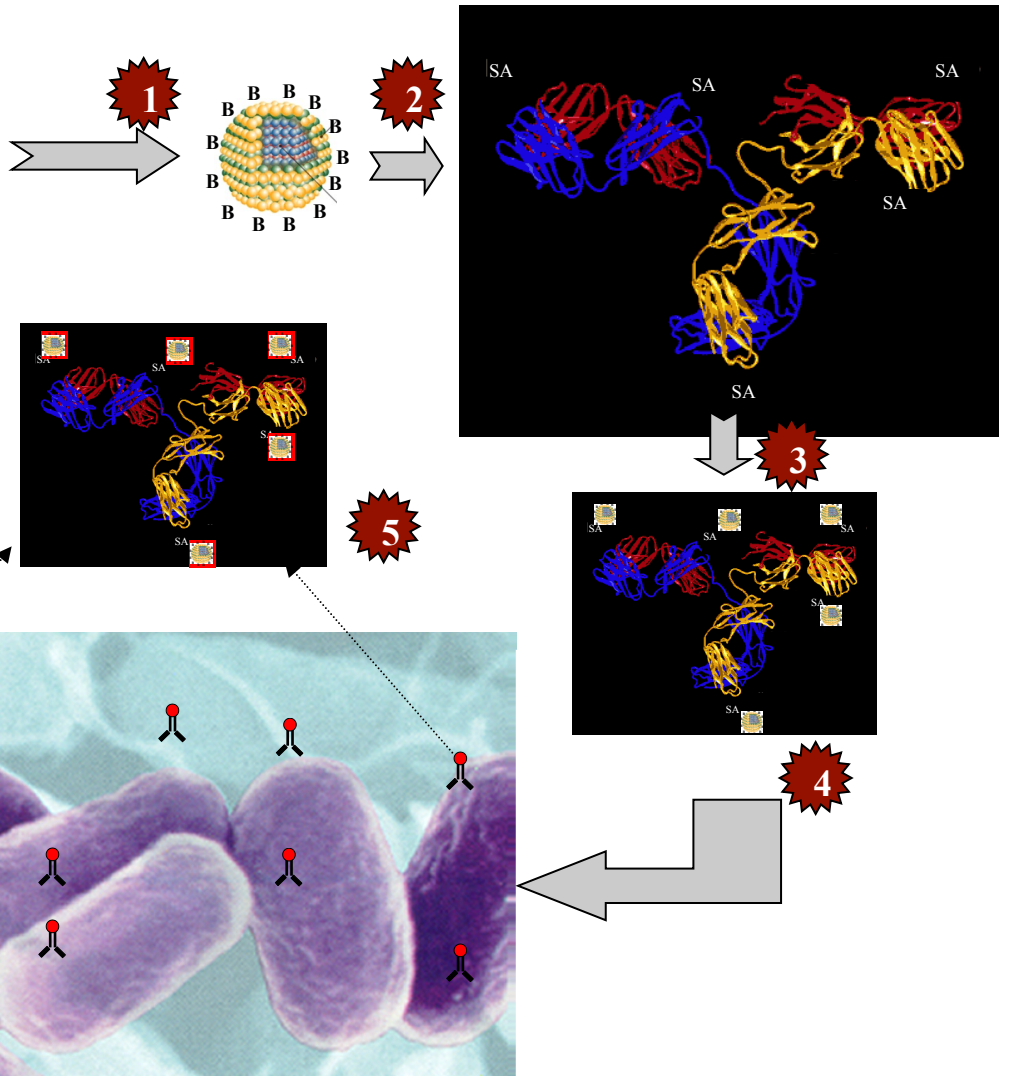

Detection of E. coli

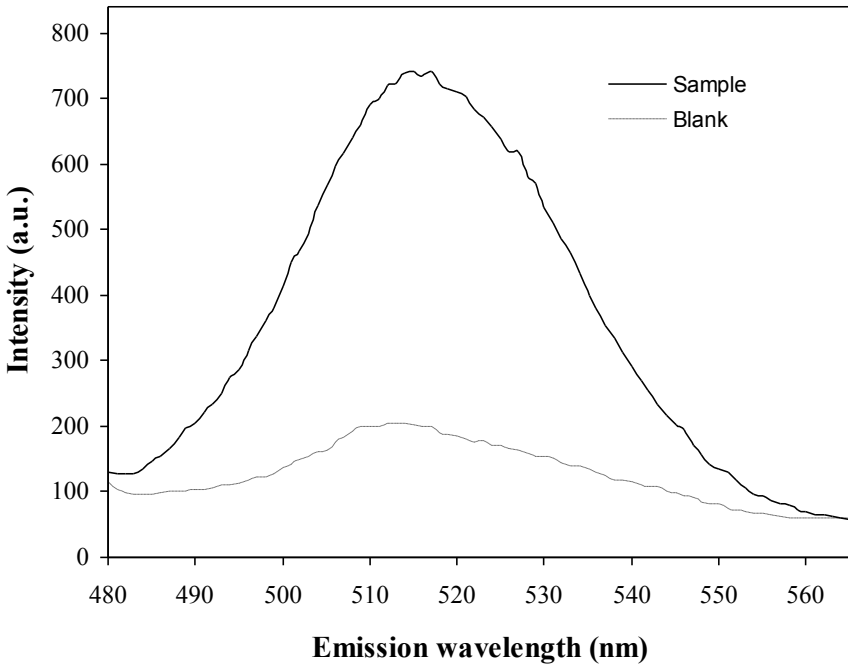

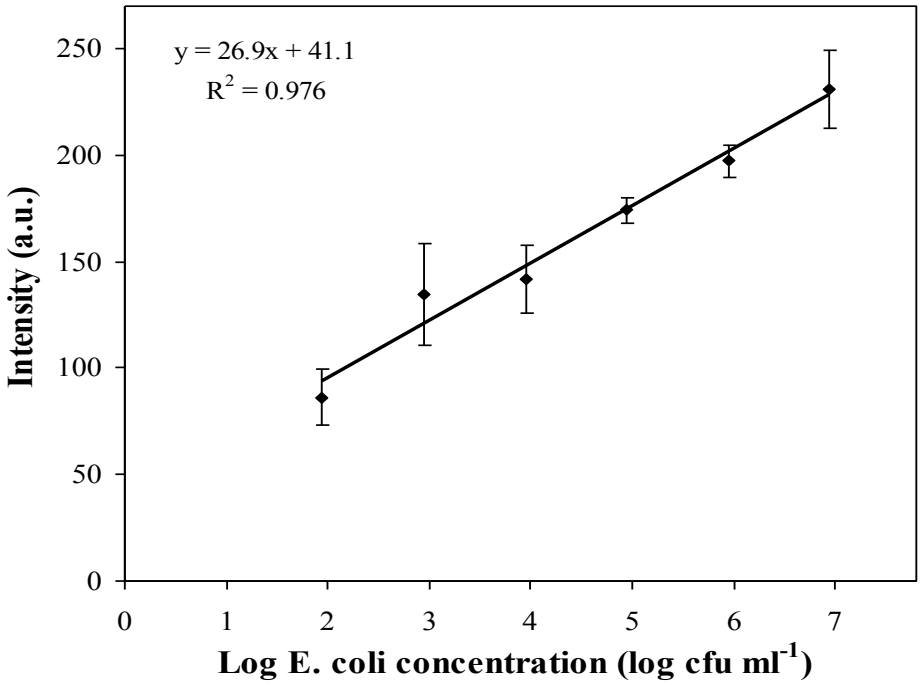

- **Total analyze time: 2 hours**

Sellectivity

E. aerogenes (5.0×10^5 kob ml^{-1}), *E. dissolvens* (1.2×10^5 kob ml^{-1}) and *E. coli* (8.9×10^5 kob ml^{-1}) varlığında ölçülen floresans intesite değerleri.

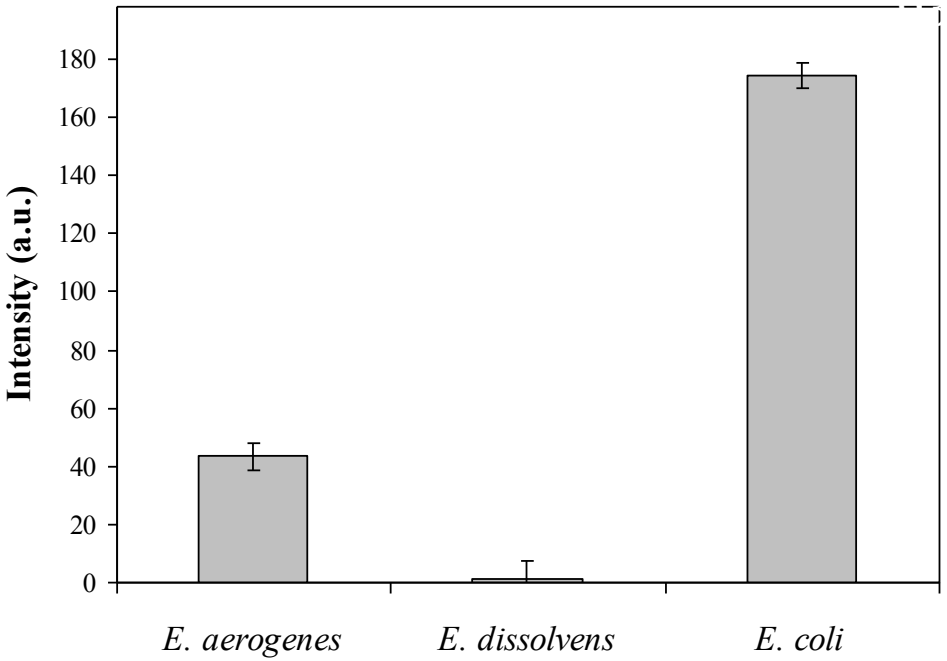

Real samples

Water samples	Developed method (cfu ml^{-1})	Referance method (cfu ml^{-1})
Lake	$3.2 \pm 3.1 \times 10^3$	$5.0 \pm 1.5 \times 10^3$
E. coli contaminated tap water	$2.0 \pm 1.1 \times 10^3$	$3.9 \pm 1.0 \times 10^3$
E. coli ve *E. aerogenes* contaminated tap water	0	$3.5 \pm 1.4 \times 10^1$

Dudak F.C., **İ.H. Boyacı**. Enumeration of Immunomagnetically Captured *Escherichia coli* in Water Samples Using Quantum Dot Labeled Antibodies, *Journal of Rapid Methods and Automation in Microbiology*, **16** (2008) 122–131.

Multiplex detection with quantum dots

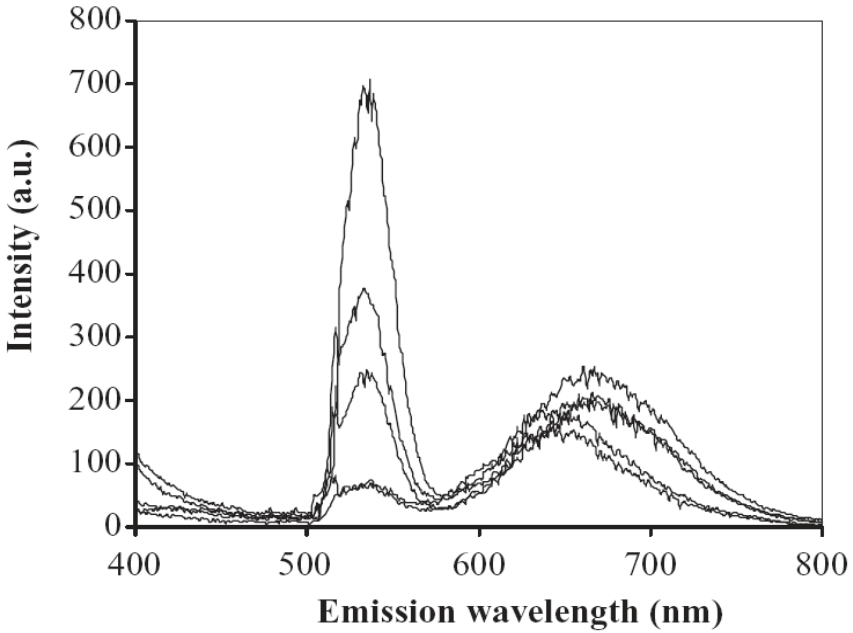

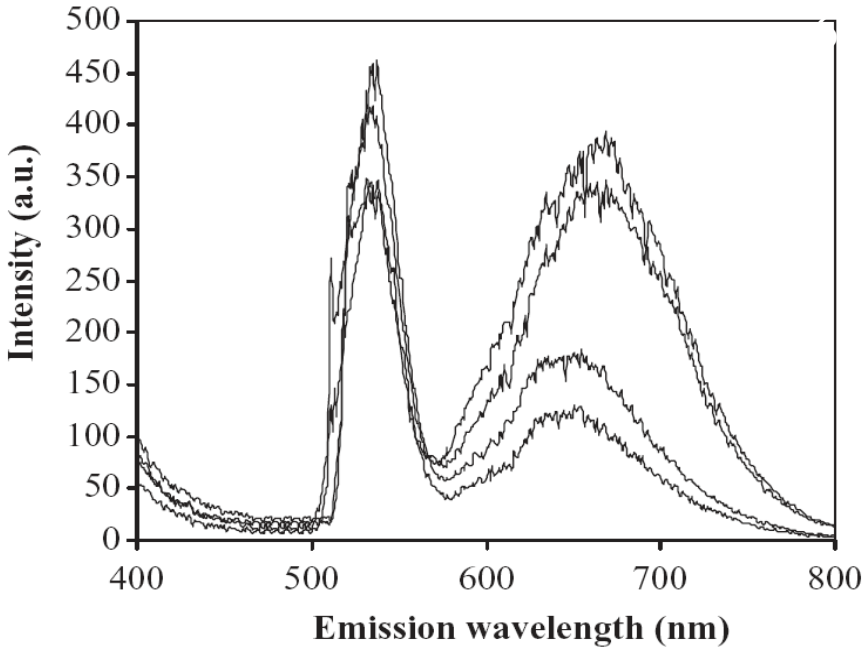

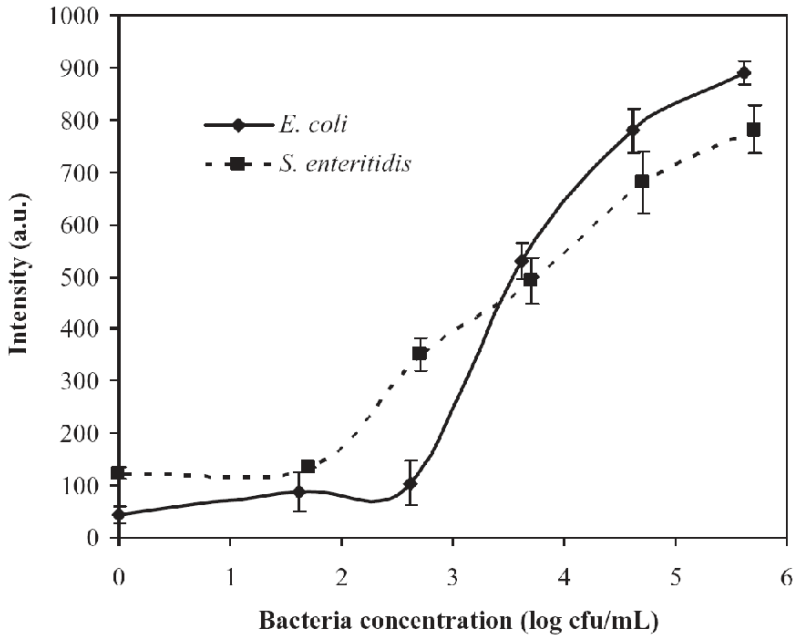

Simultaneous detection of *Escherichia coli and Salmonella enteridis* using quantum dots
excitation wavelength: 240 nm
emission wavelength s: 537 nm ve 660 nm

Dudak F.C., İ.H. Boyacı, Multiplexed detection of *Escherichia coli* and *Salmonella enteritidis* by using quantum dot labeled antibodies, *Journal of Rapid Methods and Automation in Microbiology* 17, 3 (2009) 315-327.

Quantitative Photoelectrochemical Detection of Biotin Conjugated CdSe/ZnS Quantum Dots on the Avidin Immobilized ITO Electrodes

Motivation;

- QDs are promising labeling agents in biosensor systems.
- QDs are widely used in fluorescence applications and electrochemical stripping assays.
- However, photoelectrochemical biosensor studies of these powerful tools are rare.

In this study;

- The light induced photocurrent generation from CdSe/ZnS (core/shell) QDs in a photoelectrochemical cell was investigated and the quantitative detection of biotin conjugated QDs was performed on the avidin immobilized ITO electrodes to perform a bioaffinity biosensor.

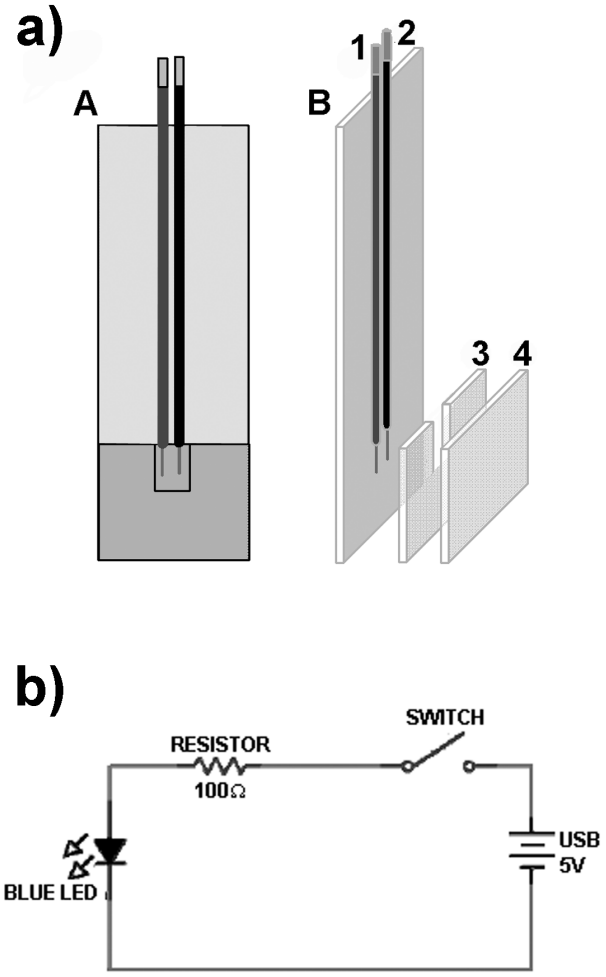

a) Design of the photoelectrochemical cell, (a) front view of the cell, (b) detached cell and its components, (1) Pt counter electrode, (2) Ag pseudo reference electrode, (3) Cell gasket (thickness = 2mm), (4) ITO coated PET working electrode; b) the LED circuit used as light source.

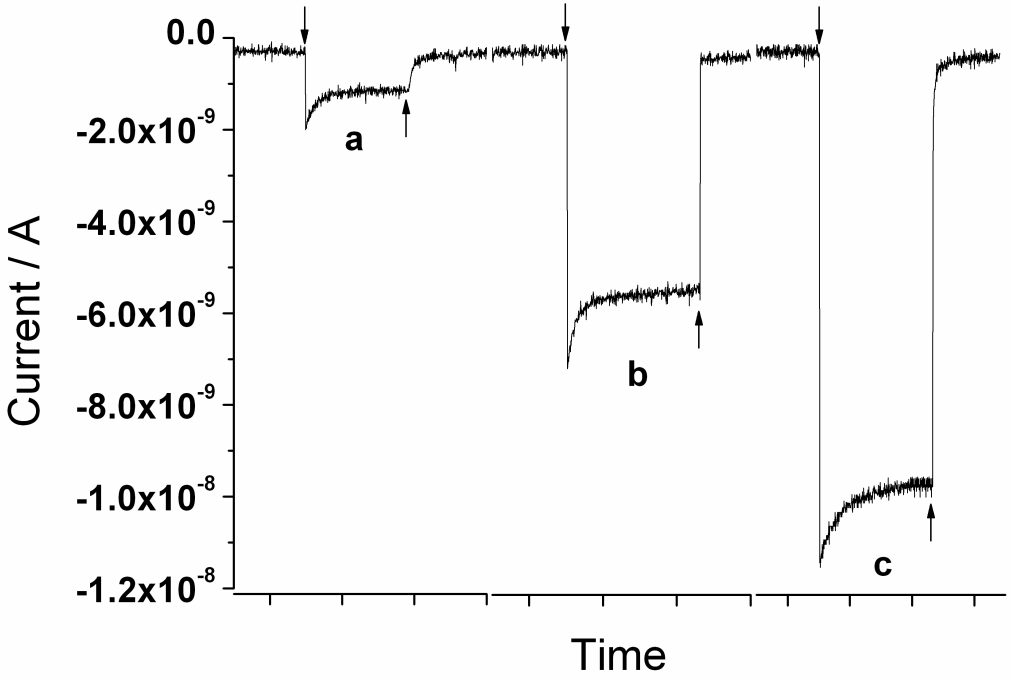

Photocurrent generated at 0.2 V vs. pseudo Ag upon illumination with a blue LED (λmax = 470 nm, Brightness: 11000 mcd) at Amine-QD concentrations a) 38 nM, b) 114 nM and, c) 227 nM. Data were obtained in 0.1 M phosphate buffer, pH 7.0. (↓ and ↑ refer to "on" and "off" states of the light source, respectively).

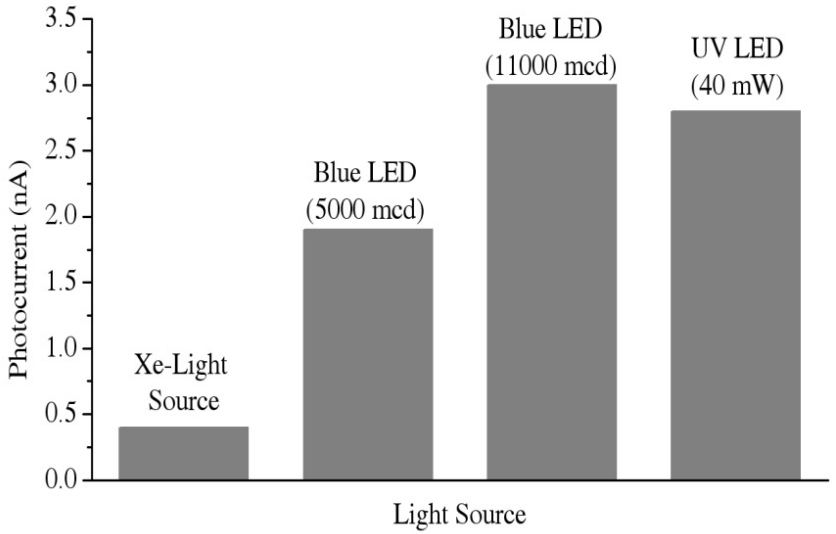

Photocurrent values obtained by illumination with different light sources. 200 mV vs. pseudo Ag, 0.1 M phosphate buffer pH 7.0

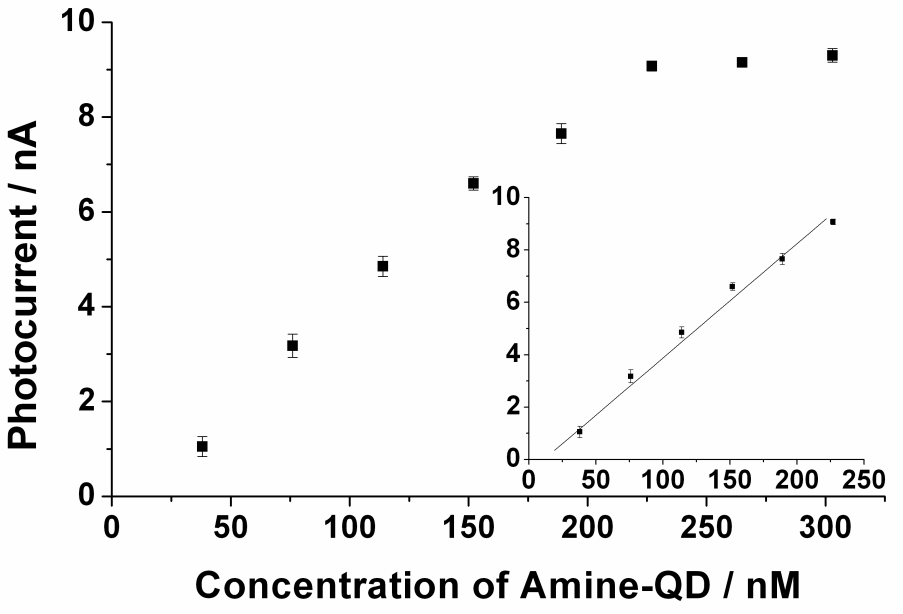

Dependence of the photocurrent on the concentration of Amine-QDs. Inset: Calibration plot (0.2 V vs. pseudo Ag, 0.1 M phosphate buffer pH 7.0).

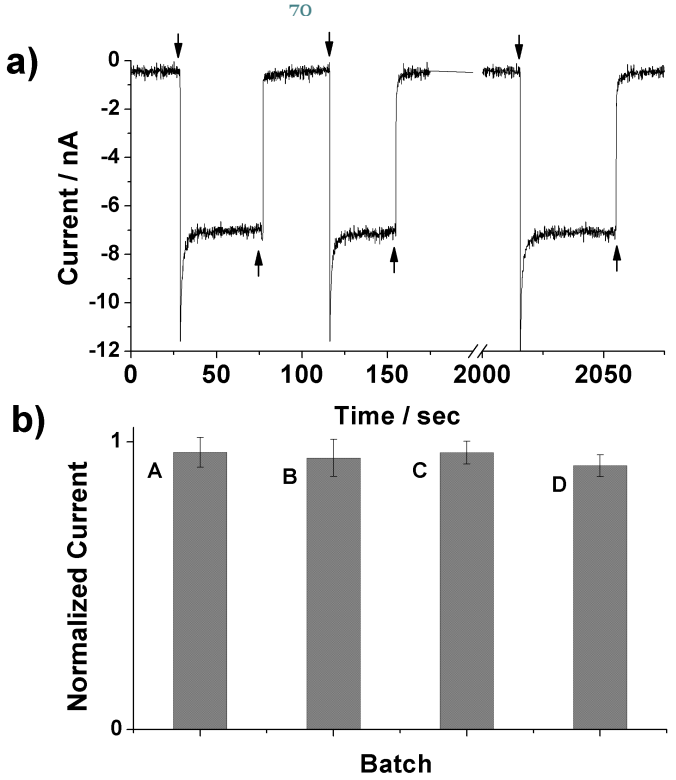

Repeatability of photocurrent response of QDs a) time based measurement b) photocurrent values for the different batches (↓ and ↑ refer to “on” and “off” states of the light source, respectively).

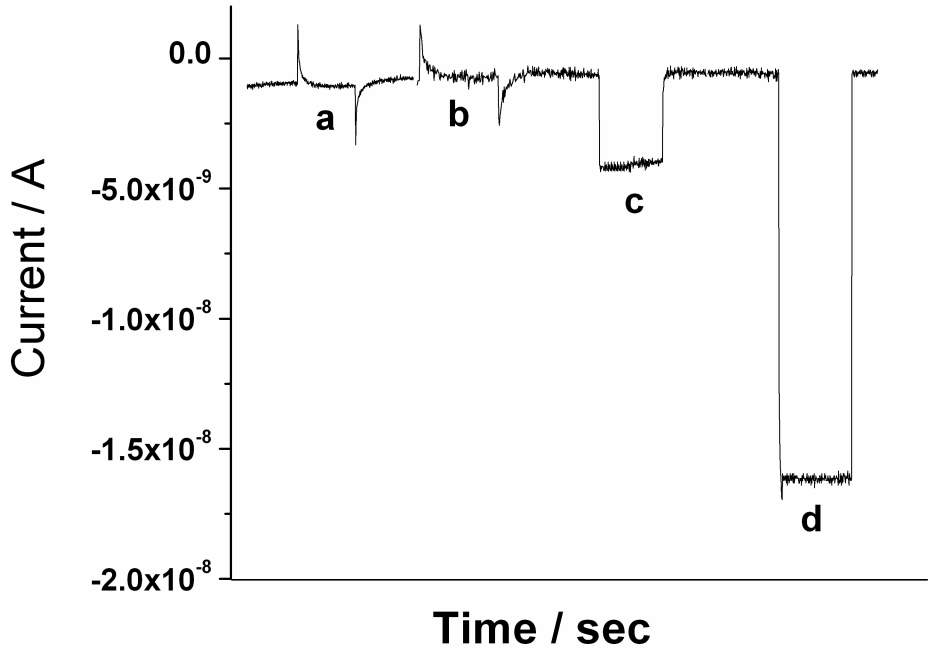

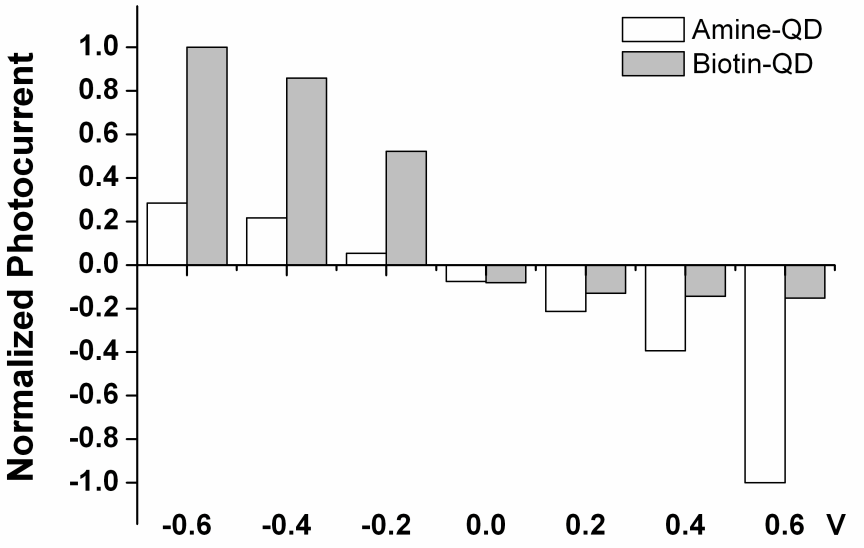

Effect of methylene blue (MB) on the photocurrent, (a) control in 0.1 M phosphate buffer (b) 12 μM MB in 0.1 M phosphate buffer (c) QD in phosphate buffer (d) QD in 12 μM MB/phosphate buffer. All measurements were performed at 0.2 V vs pseudo Ag.

Direction of the photocurrent of Amine–QDs and Biotin-QDs (0.1 M phosphate buffer, pH 7.0).

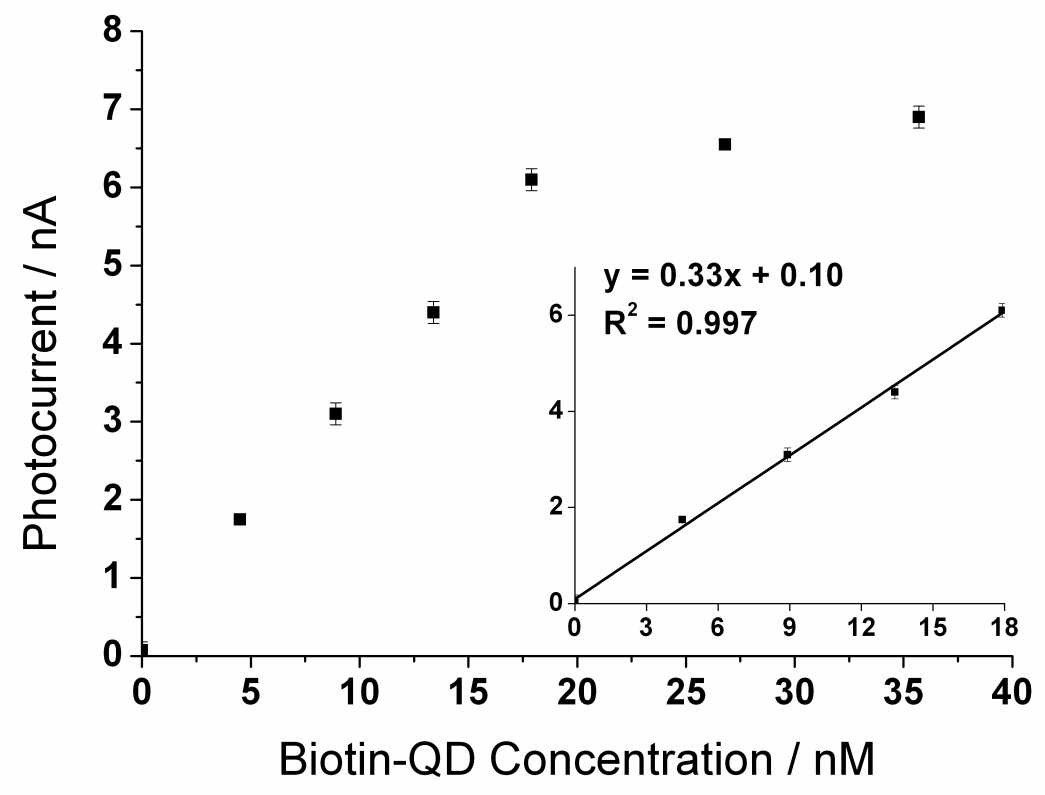

Photocurrent response as a function of Biotin-QD concentration reacted with the avidin-immobilized ITO electrodes (0.1 M phosphate buffer (pH 7.0), 12 μM MB, -0.4 V vs. pseudo Ag).

Conclusion

- *A linear calibration graph was obtained* in the range of 4 and 18 nM of biotin conjugated QDs with a coefficient of determination of 0.997.
- Results imply that QDs can be successfully used as photoelectroactive labels for the photoelectrochemical biosensor systems.

DNA detection

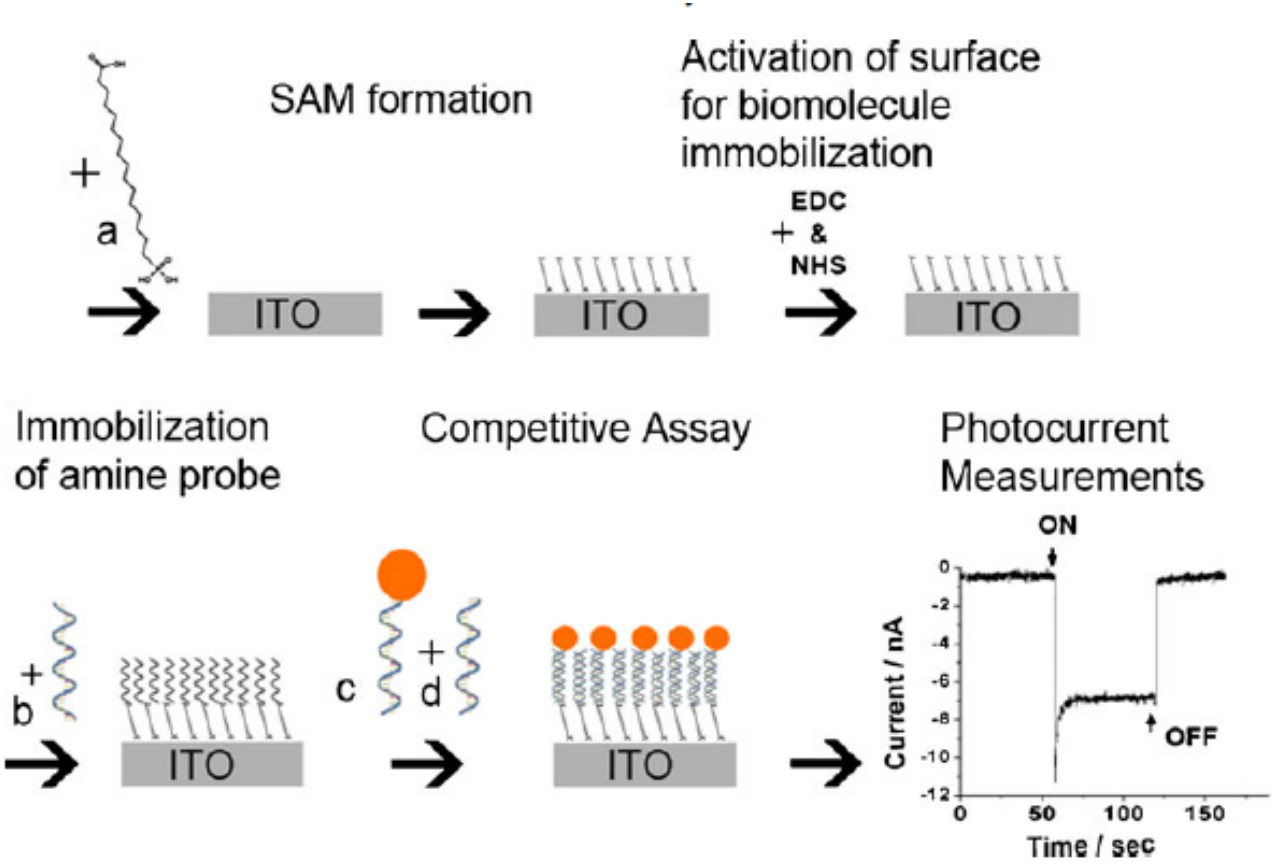

Scheme 1 Schematic representation of self-assembled monolayer formation, surface activation, probe immobilization and the competitive DNA assay. **a** 16-phosphonohexadecanoic acid, **b** amine-modified ssDNA (probe), **c** QD-ssDNA conjugate and **d** target ssDNA (*ON* and *OFF* refers to states of the light source)

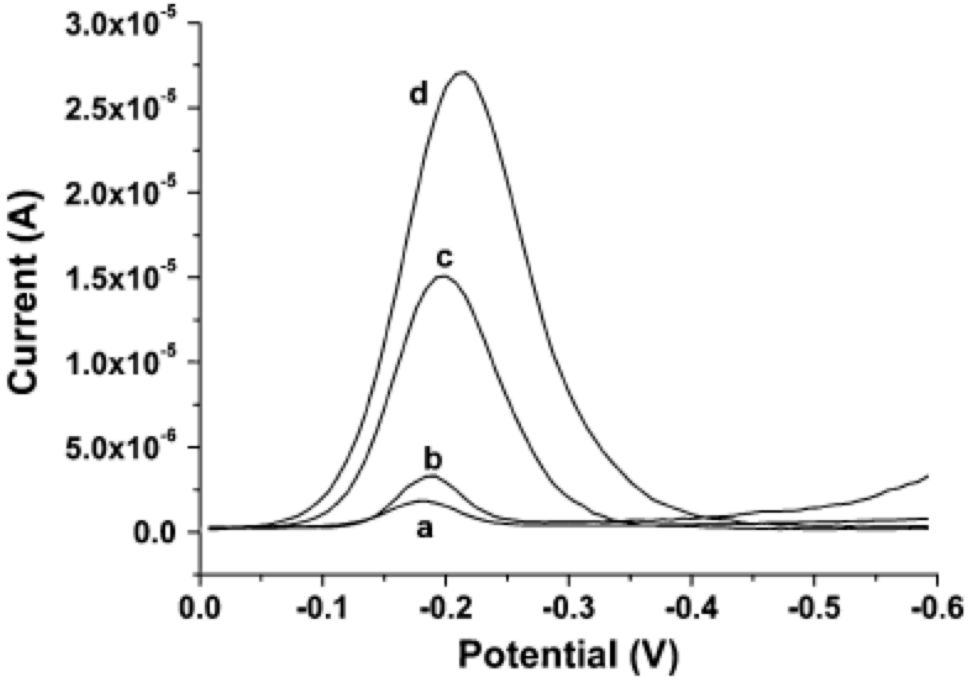

Fig. 1 Differential pulse voltammetry of MB at different electrodes: **a** SAM/ITO, **b** Bare ITO, **c** after hybridization on DNA-modified ITO electrode, and **d** before hybridization on DNA-modified ITO electrode

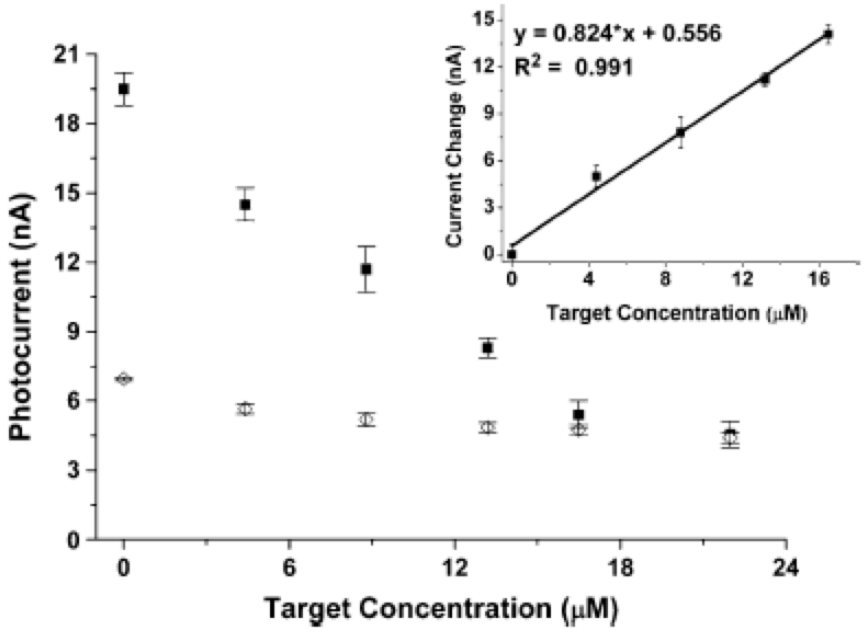

Fig. 3 Photocurrent values for the competitive hybridization assays performed at 25 °C (*open diamond*) and 50 °C (*filled square*). *Inset* linear dependence of current change on the target ssDNA at 50 °C. The *error bars* refer to standard deviation of repetitive measurements (n=3)

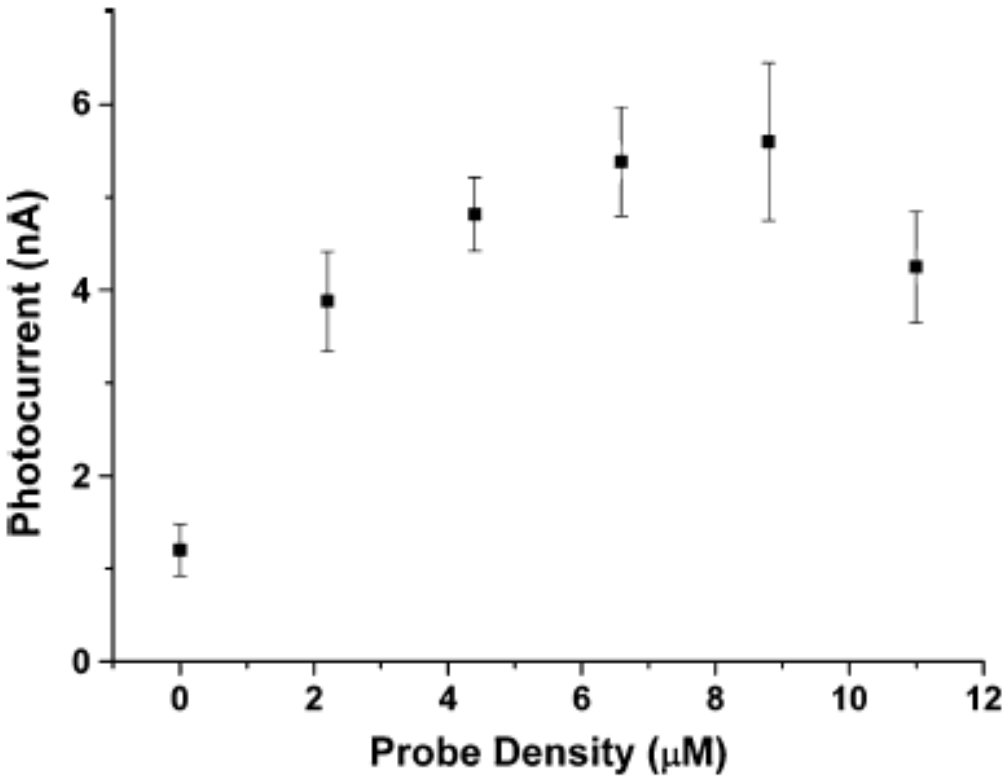

Fig. 2 Effect of probe density on the hybridization efficiency. The *error bars* refer to standard deviation of repetitive measurements (n=3)

Bas D., I.H. Boyaci, Photoelectrochemical competitive DNA hybridization assay using semiconductor quantum dot conjugated oligonucleotides, Anal Bioanal Chem (2011) 400:703–707.

Surface plamon resonance (SPR)

Bacteria detection

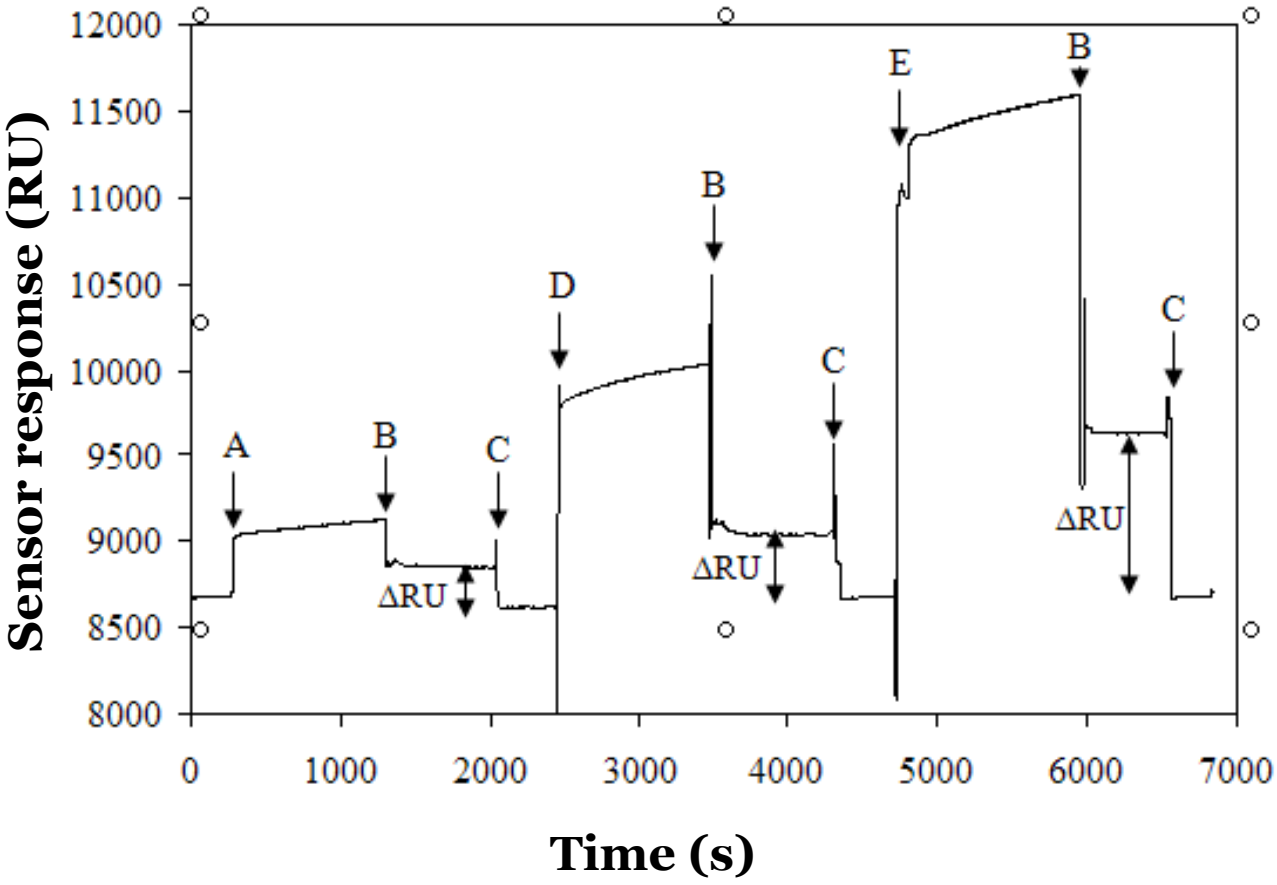

- A) *E. coli* sample (9.0×10^{1} cfu ml^{-1});
- B) PBS;
- C) 1% SDS solution;
- D) *E. coli* sampel (1.8×10^{3} cfu ml^{-1});
- E) *E. coli* sample (1.8×10^{5} cfu ml^{-1}).

Calibration graph

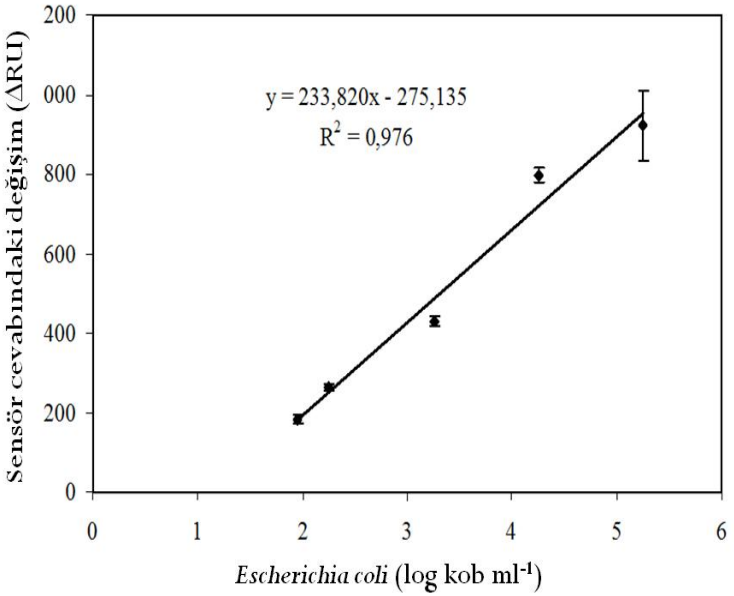

Reuseability

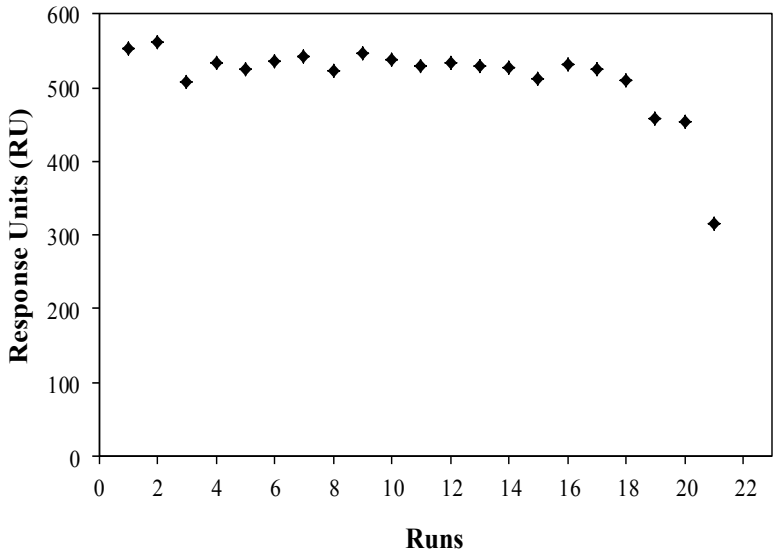

Sellectivity

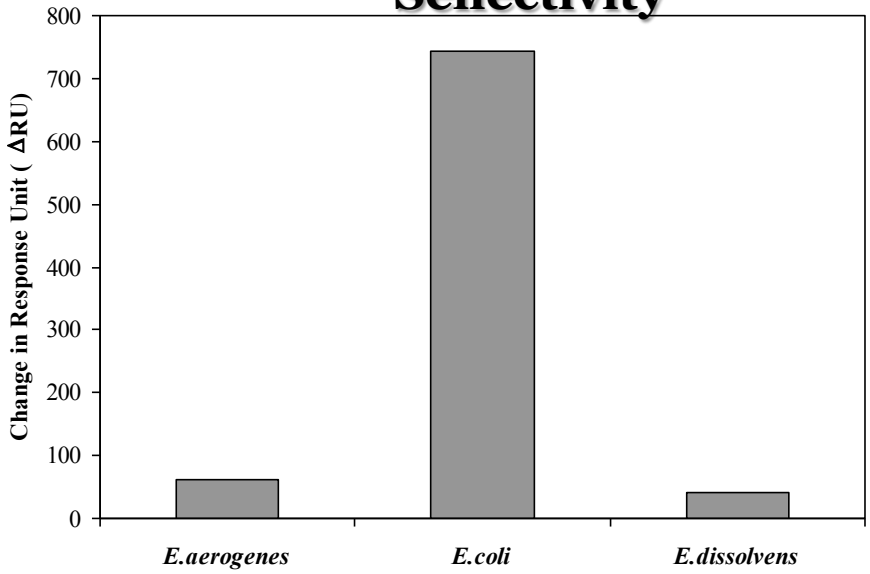

E. aerogenes (1.8×10^5 cfu/ml)
E. dissolvens (1.4×10^4 cfu/ml)
E. coli (1.8×10^4 cfu/ml).

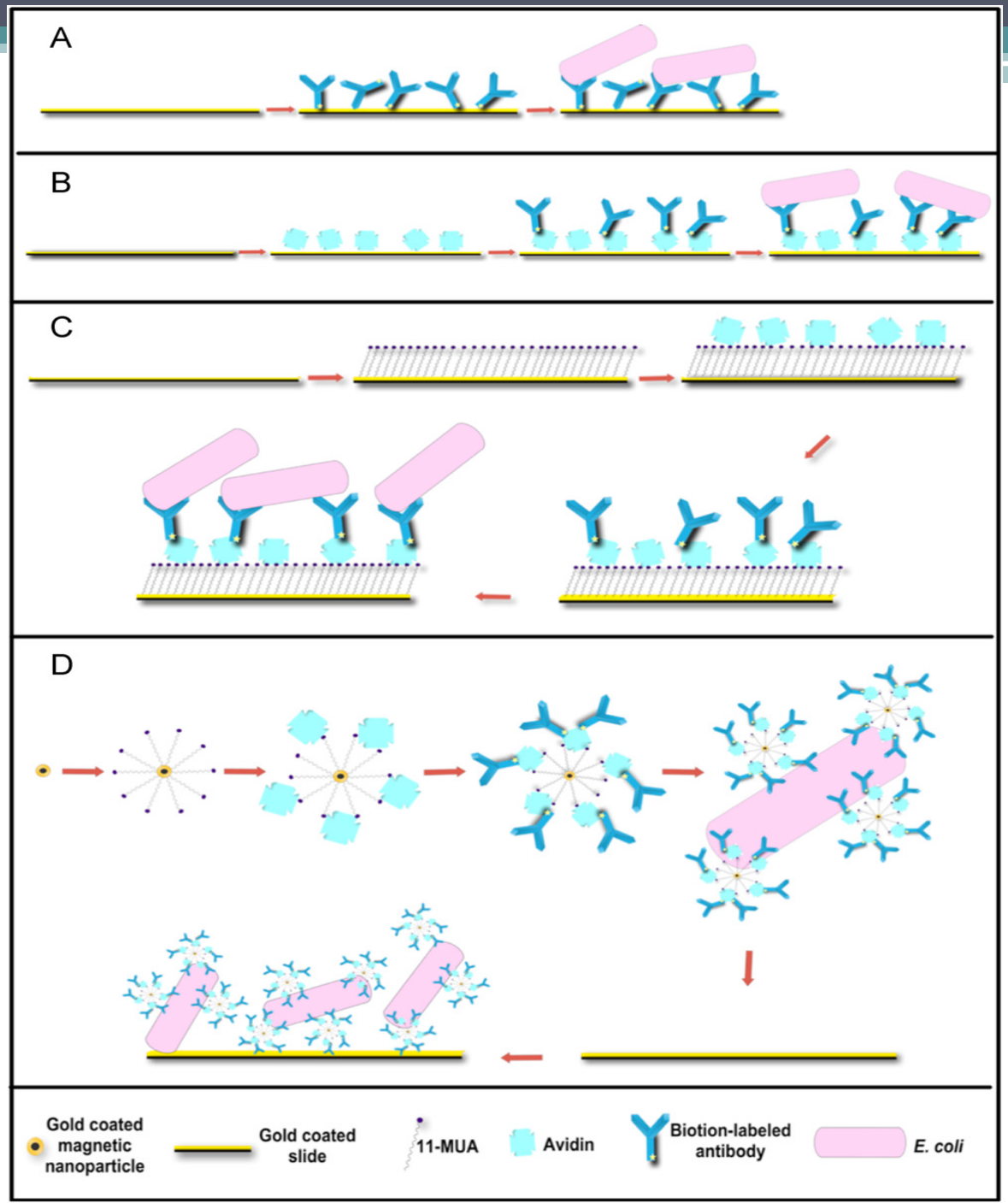
A
B
C
D
Gold coated magnetic nanoparticle
Gold coated slide
11-MUA
Avidin
Biotion-labeled antibody
E. coli

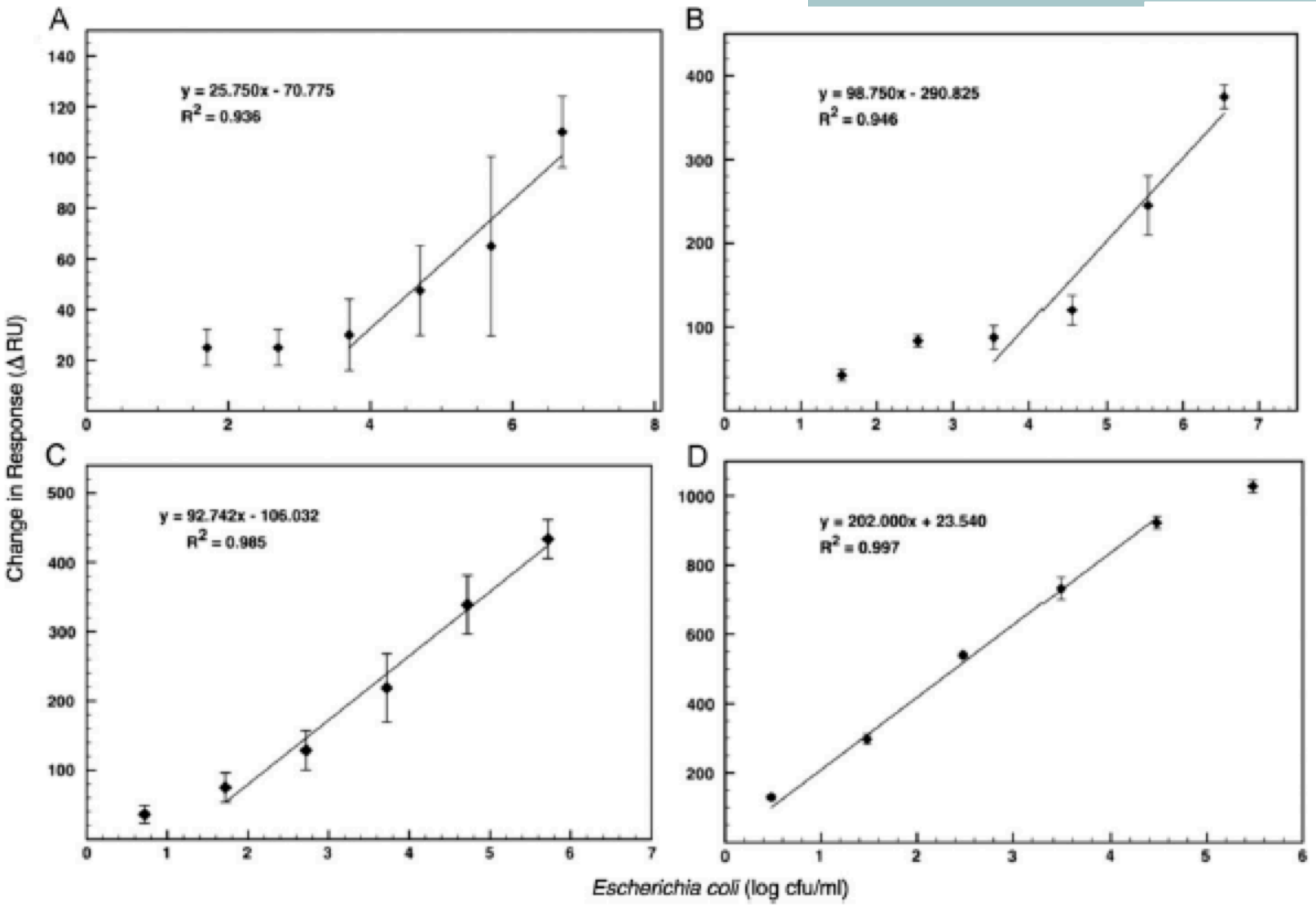

Fig. 2. Calibration curves for *E. coli* obtained with SPR systems based on the (A) non-specific adsorption of antibodies, (B) specific adsorption of antibodies via avidin–biotin interaction, (C) SAM formation and (D) using of magnetic gold nanoparticles.

Table 1
Comparison of the methods.

Principle of the strategy	Working range (cfu/ml)	Slope of the calibration curve	LOD (cfu/ml)
Non-specific adsorption	5.5×10^3–5.5×10^6	25.3	4.8×10^5
Specific adsorption	3.5×10^3–3.5×10^6	98.8	6.2×10^3
SAM formation	5.2×10^1–5.2×10^5	92.7	35
Using of nanoparticles	3.0×10^0–3.0×10^4	209.1	3

Acknowledgements

- These studies supported by
  - The Scientific and Technological Research Council of Turkey;
    - Project Number: 107T682-COST MP0701.
    - Project Number: 108 O 031-COST Action MP0803.
    - Project Number: 108 T 794-COST Action MP0901.
    - Project Number: 111 T 096-COST Action TD1102.
  - Hacettepe University, Scientific Research Center
    - Project number: 01 02 602 009.